REVIEWS OF GEOPHYSICS, VOL. 26, NO. 4, PAGES 761–780, NOVEMBER 1988

A Review and Comparative Evaluation of Multilevel Boundary Layer Parameterizations for First-Order and Turbulent Kinetic Energy Closure Schemes

TEDDY HOLT AND SETHU RAMAN

Department of Marine, Earth and Atmospheric Sciences, North Carolina State University, Raleigh

Multilevel parameterizations of the atmospheric boundary layer using first-order and turbulent kinetic energy (TKE) closure schemes are reviewed. Eleven schemes, chosen as representative of both first-order and TKE closure, are then used for comparison in a one-dimensional barotropic planetary boundary layer model. TKE closure schemes evaluated are the E-ε schemes in which eddy viscosity K_m is determined from turbulent kinetic energy and energy dissipation ε and the l model schemes in which K_m is determined from TKE and mixing length l. Comparison of model simulations of mean and turbulence structure for first-order closure and TKE closure schemes to observational data (MONEX79) is given. The two main conclusions drawn from this comparison are that (1) the mean structure of the boundary layer is fairly insensitive to the type of closure scheme, given that the scheme properly accounts for turbulent boundary layer mixing, and (2) TKE closure is preferable to first-order closure in predicting the overall turbulence structure of the boundary layer. Among the TKE schemes compared in this paper, the modified Detering and Etling (1985) scheme is preferred.

1. INTRODUCTION

Much has been written in recent years concerning modeling and parameterizations of the planetary boundary layer (PBL), particularly in review works [e.g., *Blackadar*, 1979; *McBean et al.*, 1979; *Wyngaard*, 1982; *Panofsky and Dutton*, 1984]. However, little has been resolved in terms of development of improved parameterizations or the direction and future progress of PBL parameterization schemes as they relate to numerical weather prediction. The effects of the boundary layer can be incorporated into a large-scale model in two ways, as first discussed by *Clark* [1970] and *Deardorff* [1972]. One way is to parameterize the entire PBL as one layer. This involves identifying and relating unresolvable processes in the PBL with resolvable ones. The complexity of this single-layer PBL parameterization lies in the variety and interdependence of atmospheric processes acting on different scales. The second approach, and the one discussed in this paper, is to include several computational levels in the PBL in order to resolve the boundary layer structure effectively and explicitly. Such multilevel PBL formulations require turbulent fluxes of momentum, heat, and moisture at several levels within the PBL. Thus they require some type of closure scheme to relate turbulent fluxes to mean quantities.

Basic closure schemes are presently limited to first, $1\frac{1}{2}$ (or turbulent kinetic energy), second, and to a lesser extent, third order. Second- and third-order schemes involve more of the physics of the boundary layer through increased formulation and numerical complexity. The intent here is to concentrate only on multilevel PBL parameterizations as they pertain to first-order and turbulent kinetic energy (TKE) closure. First-order closure is well documented, but there has not been a good review of TKE closure. In section 2 we present a review of past work on various multilevel parameterizations. Representative parameterizations of the first-order and TKE closure schemes are then selected for comparison using a one-dimensional model.

Observational data of the mean and turbulent structure of the marine boundary layer will be compared to model results in section 3. The data set used is from the Monsoon Experiment (MONEX79). It represents a unique opportunity to study turbulent structure of a marine boundary layer in a region in which relatively weak sea surface temperature gradients existed. The baroclinicity of the region and the effects of the barotropic assumption in the one-dimensional (1-D) model are important and will also be considered in section 3.

2. REVIEW OF CLOSURE SCHEMES

2.1. *First-Order Closure*

The closure problem arises from representing the total turbulent flow in the atmosphere in terms of the mean flow. The fundamental concern is not to introduce more unknowns into the equations describing the atmosphere such that the number of unknowns exceeds the number of equations. The principle behind the simplest way of closing the system of equations, first-order closure, as originally proposed by *Boussinesq* [1877], is to model turbulent transfer as molecular transport as follows:

$$-(\overline{uw}, \overline{vw}) = K_m(\partial U/\partial z, \partial V/\partial z)$$
$$-(\overline{w\theta}) = K_h(\partial \Theta/\partial z) \qquad (1)$$
$$-(\overline{wq}) = K_q(\partial Q/\partial z)$$

where $\overline{uw}$, $\overline{vw}$, $\overline{w\theta}$, and $\overline{wq}$ represent vertical turbulent fluxes and K_m, K_h, and K_q are eddy viscosity coefficients of momentum, heat, and moisture, respectively. This is the fundamental premise of first-order closure, that these unknowns, turbulent fluxes $\overline{uw}$, $\overline{vw}$, etc. (for first-order closure) are related to mean vertical gradients by an eddy viscosity coefficient K which is a property of the turbulent flow. It is this eddy viscosity coefficient which must account for the complexities of turbulence. The problem of first-order closure is then effectively reduced to the problem of resolving K, and this is the problem addressed here.

Paper 88RG03114.
8755-1209/88/88RG-03114$05.00

TABLE 1. K Profiles

Author	K Profile	Range of Validity	Constants
O'Brien [1970]	$K_m = K(h) + [(z-h)^2/(h-z_s)^2]\{K(z_s) - K(h) + (z-z_s)[\partial K/\partial z_s + [2(K(z_s) - K(h))/(h-z_s)]]\}$	all Ri $z_s < z < h$	
Yamamoto et al. [1973]	$K_m = k^2z^2[S + (g/\theta\lvert\partial\theta/\partial z\rvert)^{1/2}]$	$\partial\theta/\partial z < 0$	$S^2 = [(\partial U/\partial z)^2 + (\partial V/\partial z)^2]$
	$K_m = k^2z^2[S - (L/2z)(\sigma g/\theta\,\partial\theta/\partial z)^{1/2}]$	$\partial\theta/\partial z > 0$	$\sigma = 15$
Orlanski et al. [1974]	$K_m = K_0[1 + C(-g\Delta\theta(\Delta z)^3/\theta K_0\nu_0)^{1/3}]$	$\Delta\theta < 0$	$K_0 = 0.0093$ m^2 s^{-1}; $C = 0.1$; Δz is local vertical grid size; $\Delta\theta$ is local θ difference $\nu_0 = 0.0093$ m^2 s^{-1}
	$K_m = K_0$	$\Delta\theta \geq 0$	
Businger and Arya [1974]	$K_m = kzu_* \exp(-fz\lvert V_g\rvert u_*^2)/(1 + \beta z/L)$	stable	$\beta = 4.7$
Pielke and Mahrer [1975]	$K_m = K(h) + [(z-h)^2/(h-z_s)]^2\{[K(z_s) - K(h)] + (z-z_s)[\partial K/\partial z_s + (2(K(z_s) - K(h))/(h-z_s))]\}$	$z_s < z < h$	
	$K_m = K(h)$	$z > h$	
	$K_m = (z/h)K(z_s)$	$z < z_s$	
Brost and Wyngaard [1978]	$K_m = kzu_*(1 - z/h)^{3/2}(1 + \beta z/L)^{-1}$	stable	$\beta = 4.7$

For completeness we include simplified equations of the one-dimensional PBL, neglecting horizontal advection terms and considering only vertical turbulent exchange:

$$\frac{\partial U}{\partial t} - fV = -\frac{\partial}{\partial z}(\overline{uw}) - \frac{1}{\rho}\frac{\partial P}{\partial x}$$

$$\frac{\partial V}{\partial t} + fU = -\frac{\partial}{\partial z}(\overline{vw}) - \frac{1}{\rho}\frac{\partial P}{\partial y} \qquad (2)$$

$$\frac{\partial \Theta}{\partial t} = -\frac{\partial}{\partial z}(\overline{w\theta}) \qquad \frac{\partial Q}{\partial t} = -\frac{\partial}{\partial z}(\overline{wq})$$

where uppercase values U, V, Θ, and Q represent mean values of east-west and north-south wind, potential temperature, and humidity, respectively. Lowercase values denote deviations from the mean. Incorporating the eddy viscosity concept (1) along with geostrophic winds (U_g, V_g) yields a set of more easily modeled equations:

$$\frac{\partial U}{\partial t} - f(V - V_g) = \frac{\partial}{\partial z}\left(K_m\frac{\partial U}{\partial z}\right)$$

$$\frac{\partial V}{\partial t} + f(U - U_g) = \frac{\partial}{\partial z}\left(K_m\frac{\partial V}{\partial z}\right) \qquad (3)$$

$$\frac{\partial \Theta}{\partial t} = \frac{\partial}{\partial z}\left(K_h\frac{\partial \Theta}{\partial z}\right) \qquad \frac{\partial Q}{\partial t} = \frac{\partial}{\partial z}\left(K_q\frac{\partial Q}{\partial z}\right)$$

where K_q is assumed equal to K_h.

Modeling of the lowest 100 m of the atmosphere is best accomplished by making use of surface layer theory. Effective and efficient parameterization schemes based on Monin-Obukhov similarity are widely used for the surface layer (see, for example, *Panofsky and Dutton* [1984], *Pielke* [1984], and *Arya* [1977]) and will not be expounded upon here. Instead we focus only on the bulk of the boundary layer away from the surface. It is this region in which nonstationarity and inhomogeneity often dominate that is most difficult to model. In this region, first-order closure schemes can be divided into two groups: one in which mixing length (l) parameterizations are used to determine K and one in which mixing length is not used. We first consider those parameterizations which do not utilize the mixing length approach but instead describe a K profile.

2.1.1. *K profile approach.* The simplest and oldest approach to first-order closure is to specify a K profile in which K is a constant. These constant K models are easily solved analytically [*Ekman*, 1905], but physically they are not well representative of the boundary layer as could be expected from their simplicity [*Krishna*, 1980]. A more physically realistic approach is to prescribe a K profile which varies with height. Thus K is allowed to depend on height, thermal stability, local gradients of potential temperature, etc. Numerous authors including *O'Brien* [1970], *Yamamoto et al.* [1973], *Businger and Arya* [1974], *Orlanski et al.* [1974], *Pielke and Mahrer* [1975], *Deardorff* [1975], *Brost and Wyngaard* [1978], and *Bodin* [1980] have considered this approach to study a variety of atmospheric conditions.

In the steady, horizontally homogeneous stable boundary layer, *Brost and Wyngaard* [1978] parameterized K based on surface layer and mixed layer scaling, while *Businger and Arya* [1974] used a scheme in which K adjusts asymptotically throughout the boundary layer (see Table 1 for a description of K profile schemes). For more general atmospheric conditions, *O'Brien* [1970] suggested a scheme, still used by some [see *Tapp and White*, 1976], in which K is obtained from a third-order polynomial determined by specified boundary conditions at the top of the boundary layer (h) and at the top of the surface layer (z_s).

Others have used schemes which utilized different subgrid scale parameterizations, such as that given by *Deardorff* [1974]. *Orlanski et al.* [1974] used a simplified two-dimensional (2-D) version of *Deardorff*'s [1974] three-dimensional (3-D) numerical model and specified K proportional only to local vertical gradients of potential temperature. *Deardorff* [1975] used a similar approach but with K proportional to the local turbulent energy. *Yamamoto et al.* [1973] assumed K proportional to both vertical wind shear and vertical gradients of potential temperature. *Pielke and Mahrer* [1975] combined *O'Brien*'s [1970] formulation with *Deardorff*'s [1974] prognostic equation for PBL height h to better resolve boundary layer growth.

All of these first-order schemes are relatively simple in that they require only routinely measured or model resolvable meteorological variables to explicitly determine K. Thus K profiles are specifically determined by parameters such as

$\partial\Theta/\partial z$, z/L, z/h, etc., where L is Monin-Obukhov length. This is a drawback in that these parameters are often not good indicators of the total turbulent flow. A slightly different approach to this type of determination of K is an approach in which K is expressed in terms of a mixing length l, such that

$$K_m = l^2[(\partial U/\partial z)^2 + (\partial V/\partial z)^2]^{1/2} \quad (4)$$

and one must determine l instead of K. This mixing length approach will now be considered.

2.1.2. *Mixing length approach.* The principle of a mixing length in terms of atmospheric turbulence dates back to the work of *Prandtl* [1932]. He reasoned, from considerations of eddy transfer, that in the surface layer, eddies move vertically at velocity w and over a distance l (or mixing length) in the process of adjusting their momentum to that of the surrounding fluid. *Blackadar* [1962], extending Prandtl's mixing length hypothesis, reasoned that l varied as kz close to the ground (where k is von Kármán's constant) but approached some constant value λ at greater heights, i.e.,

$$l = kz/(1 + kz/\lambda) \quad (5)$$

Blackadar suggested λ equal to $2.7 \times 10^{-4}|G|/|f|$ where G is the geostrophic wind and f is the Coriolis parameter. Others have used Blackadar's parameterization, or slight modifications of it, in their own schemes for determining K (see Table 2). For example, *Carlson and Foster* [1986] used an eddy viscosity turbulence model in a 2-D simulation of unstable boundary layer flow over valleys in which mixing length was Blackadar's formulation modified to include stability effects. Earlier works [*Karlsson*, 1972; *Clarke*, 1974; *Estoque and Bhumralkar*, 1970] used Blackadar's parameterization with modifications included in K profiles to account for stability (Table 2). *Djolov* [1973] utilized a modified Blackadar formulation by including the stability function ϕ_m:

$$l = kz/(\phi_m + kz/\lambda) \quad (6)$$

where $\lambda = 4.0 \times 10^{-4}|G|/|f|$ and ϕ_m is determined by the usual Businger-Dyer relationships. *Delage* [1974] used a local Monin-Obukhov length approach and *Bodin* [1976] a "neutral" mixing length approach modified by the depth of the boundary layer to extend Djolov's work to the stable boundary layer. *Lacser and Arya* [1986] summarized many of these works and provided a review of mixing length parameterizations in the stably stratified nocturnal boundary layer.

Other parameterizations of mixing length l exist. For simulating a horizontally homogeneous stratus-filled boundary layer, *Tag and Payne* [1987] used a 3-D PBL model that incorporated the mixing length parameterization first proposed by *Rossby and Montgomery* [1935]. In this scheme, l is separated into a region within the surface layer and a region above it. Mixing length is then a function of distance from the surface, as well as stability, in both regions. A scheme developed to account for stability similar to that of earlier authors [*Estoque and Bhumralkar*, 1970; *Karlsson*, 1972] is a modified *Djolov* [1973] scheme. In this scheme, l is a function of ϕ_m as earlier, but now K_m is also a function of Richardson number (see Table 2).

2.2. *Turbulent Kinetic Energy Closure*

An improvement to the simplicity of first-order closure would be a closure scheme in which more of the physics of the atmosphere is taken into account in the formulation of the eddy viscosity coefficient K. Such a scheme is the turbulent kinetic energy closure. It is essentially a first-order scheme in that closure is accomplished by means of (1), but the K coefficient is determined from more involved and hopefully more physically realistic relationships given by prognostic equations for turbulent kinetic energy and energy dissipation or mixing length. This type of closure is also more economical as compared to higher-order closure schemes. For example, second-order closure requires the integration of at least 15 partial differential equations when moisture is included. Simple first-order closure generally requires only the four equations given in (3). TKE closure requires only two additional equations, a total of six, and thus provide a more physically realistic solution to the closure problem than does first-order closure, without the involved numerical complexity of second-order closure. Thus it is often termed $1\frac{1}{2}$-order closure [*Mellor and Yamada*, 1974].

The foundation of TKE closure is the budget of turbulent kinetic energy. It is essentially a first-order closure scheme, so it does involve the same parameterization of K given in section 2.1. Here we also consider the same basic equations for the description of the atmosphere as in section 2.1 for consistency. However, an additional equation is introduced which computes the turbulent kinetic energy budget in the boundary layer. For turbulent kinetic energy E expressed as $(\overline{u^2} + \overline{v^2} + \overline{w^2})/2$, the prognostic equation for TKE over a horizontally homogeneous surface is derived as (see, for example, *Monin and Yaglom* [1971])

$$\frac{\partial E}{\partial t} = -\overline{uw}\frac{\partial U}{\partial z} - \overline{vw}\frac{\partial V}{\partial z} + \frac{g}{\Theta}\overline{w\theta} - \frac{\partial}{\partial z}\left(\overline{wE} + \frac{\overline{pw}}{\rho}\right) - \varepsilon \quad (7)$$

where the first two terms on the right-hand side (r.h.s.) represent shear production, the third term represents buoyancy production, the fourth turbulent transport, and the fifth dissipation of turbulent energy. In this closure scheme, several terms on the r.h.s. must be parameterized. The shear terms, of course, are related to mean gradients by (1). Similarly, heat flux $\overline{w\theta}$ in the buoyancy term is generally expressed as

$$-\overline{w\theta} = K_h(\partial\Theta/\partial z - \gamma_{cg}) = K_h(\partial\Theta_{cg}/\partial z) \quad (8)$$

where γ_{cg} ($=7.0 \times 10^{-4}$ K/m) incorporates countergradient heat flux [*Deardorff*, 1966]. The turbulent transport term is composed of vertical turbulent transport $\partial/\partial z\,(\overline{wE})$ and pressure transport $\partial/\partial z\,(\overline{pw}/\rho)$. The two terms are generally included as one and modeled as [*Monin and Yaglom*, 1971; *Shir*, 1973; *Rodi*, 1980]

$$-(\overline{wE} + \overline{pw}/\rho) = C(K_m\,\partial E/\partial z) \quad (9)$$

where C is a constant. Substitution of these parameterizations into (7) yields

$$\frac{\partial E}{\partial t} = K_m\left[\left(\frac{\partial U}{\partial z}\right)^2 + \left(\frac{\partial V}{\partial z}\right)^2\right] + \frac{g}{\Theta}K_h\frac{\partial\Theta_{cg}}{\partial z} + C\frac{\partial}{\partial z}\left(K_m\frac{\partial E}{\partial z}\right) - \varepsilon \quad (10)$$

Parameterization of the final term, energy dissipation ε, can be achieved either diagnostically or prognostically and will be considered in the following sections.

To organize and to clarify the different TKE closure schemes, we now separate them into three basic model schemes based on the prognostic variables considered. Basic equations, assumptions, and recent work on each parameterization will then be evaluated.

TABLE 2. Mixing Length Parameterizations

Author	K	l	Range of Validity	Constants
Blackadar [1962]	$K_m = l^2S$	$l = kz/(1 + kz/\lambda)$	all Ri	$\lambda = 2.7 \times 10^{-4}(\lvert G\rvert/\lvert f\rvert)$
Estoque and Bhumralkar [1970]	$K_m = l^2S(1 + Ri)$	$l = kz/(1 + kz/\lambda)$	$Ri > 0$	$\lambda = 2.7 \times 10^{-4}(\lvert G\rvert/\lvert f\rvert)$
	$K_m = l^2S(1 - \alpha Ri)^{-1}$		$Ri < 0$	$\alpha = 3.0$
Karlsson [1972]	$K_m = l^2S(1 + \alpha Ri)^{-2}$	$l = kz/(1 + kz/\lambda)$	$\partial\theta/\partial z \geq 0$	$\lambda = 2.7 \times 10^{-4}(\lvert G\rvert/\lvert f\rvert)$
	$K_m = K_m(1 + \alpha Ri)^{-1}$			$\alpha = 3.0$
Clarke [1974]	$K_m = l^2S(1 - \gamma\sigma)$	$l = kz/(1 + kz/\lambda)$	$\partial\theta/\partial z < 0$	$\lambda = 2.7 \times 10^{-4}(\lvert G\rvert/\lvert f\rvert)$
	$K_m = l^2S(1 - \sigma)^{-1}$		$\partial\theta/\partial z > 0$	$\gamma = 18$
				$\sigma = \dfrac{(gl)^{1/2}}{\theta}\dfrac{\partial\theta}{\partial z}S^{-1}$
Djolov [1973]	$K_m = l^2S$	$l = kz/(\phi_m + kz/\lambda)$	$\partial\theta/\partial z \geq 0$	$\phi_m = 1 + 4.7(z/L)$
			$\partial\theta/\partial z < 0$	$\phi_m = [1 - 15(z/L)]^{-1/4}$
Modified *Djolov* [1973]	$K_m = l^2S(1 - Ri)^{1/2}$	*Djolov* [1973]	$Ri < 1$	
	$K_m = 0$		$Ri \geq 1$	
Delage [1974]	$K_m = l^2S$	$\dfrac{1}{l} = \dfrac{1}{kz} + \dfrac{1}{\lambda} + \dfrac{\beta}{kL}$	$\partial\theta/\partial z \geq 0$	$\beta = 4.7$
				$\lambda = 4.0 \times 10^{-4}\lvert G\rvert/\lvert f\rvert$
Bodin [1976]	$K_m = l^2S$	$\dfrac{1}{l} = \dfrac{1}{l_n} - \left[\dfrac{1}{h}\left(\dfrac{1 + 1.32z/h}{0.001 + (kz/h)}\right)\cdot\left(\dfrac{1}{1 - 50L_0/h}\right)\right]$	$\partial\theta/\partial z < 0$	L_0 is surface M-0 length
				$l_n = \dfrac{1}{\dfrac{1}{kz} + \dfrac{1}{0.2h}}$; stable
				$h = 0.1u_*\lvert f\rvert$
				$\phi_m = (1 - 16z/L)^{-1/4}$
Carlson and Foster [1986]	$K_m = l^2S$	$l = \dfrac{k(z + z_0)/\phi_m}{1 + [k(z - z_S)/\lambda\phi_m]}$	$z > z_S$	
		$l = k(z + z_0)/\phi_m$	$z \geq z_S$	$\lambda = 100$ m
			$L \leq 0$	
Tag and Payne [1987]	$K_m = l^2\left[\dfrac{(\mathrm{DEF})^2}{2} - \dfrac{g}{\theta_0}\dfrac{K_h}{K_m}\dfrac{\partial\theta_v}{\partial z}\right]^{1/2}$	$l = \dfrac{k}{\phi_m}(z + z_0)$	$z \leq z_S$	$\mathrm{DEF} = \left[2\left(\dfrac{\partial u}{\partial z}\right)^2 + 2\left(\dfrac{\partial v}{\partial z}\right)^2 + 4\left(\dfrac{\partial w}{\partial z}\right)^2\right]$
		$l = \dfrac{k}{\phi_m}\left[(z_S + z)\left(\dfrac{h - z}{h - z_S}\right)\right]$	$z_S < z \leq h$	$z_s = 0.062\,u_*/f$
				$h = 16.0\,z_s$

$S^2 = [(\partial U/\partial z)^2 + (\partial V/\partial z)^2]$.

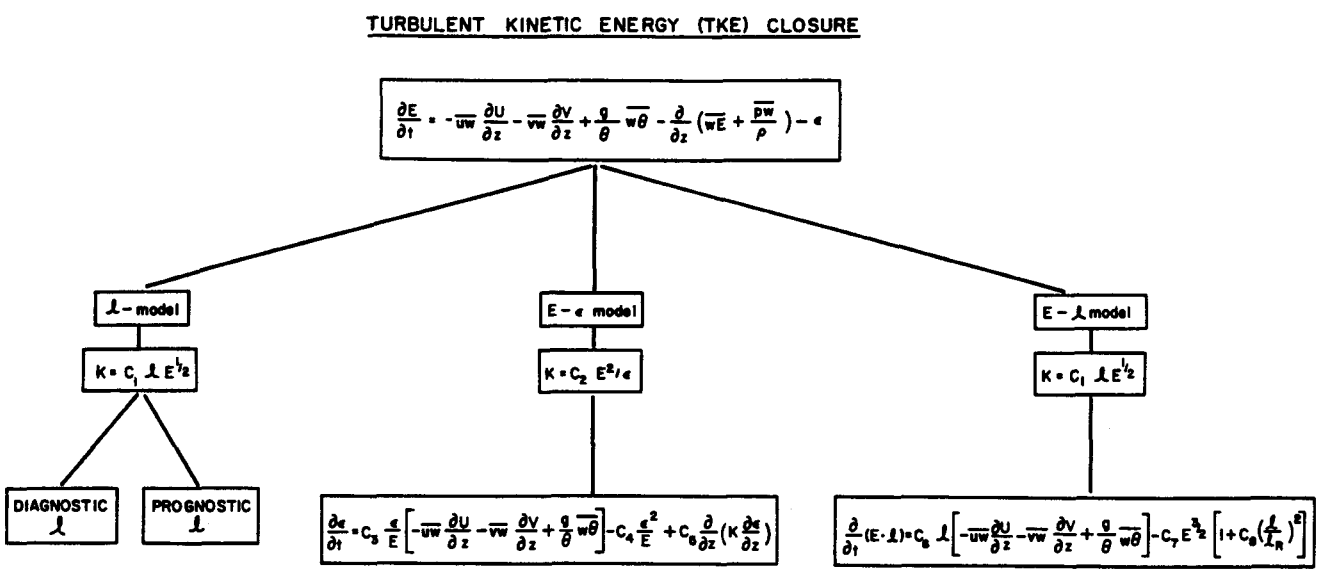

Fig. 1. Model parameterizations based on turbulent kinetic energy closure.

The first TKE parameterization considered is the "l model," in which mixing length l is modeled either diagnostically or prognostically. The second is the "E-ε model," in which a prognostic equation for ε is developed. The final approach considered is the "E-l model," in which a prognostic equation for the product $E \cdot l$ is used. This scheme is often referred to as q^2-l closure (or a level 2.5 model), where $(q^2/2)$ is the TKE [*Mellor and Yamada*, 1974] (see Figure 1).

2.2.1. *The l model.* The basis of the l model is derived from the Prandtl-Kolmogorov hypothesis [see *Monin and Yaglom*, 1971] relating eddy viscosity to turbulent kinetic energy:

$$K_m = C_1 l E^{1/2} \tag{11}$$

Constant C_1 is taken as 0.4. With turbulent energy E evaluated by a prognostic equation (7), the determination of K is again, as in the mixing length approach, determined by l. Research in l models has been divided into prognostic versus diagnostic determination of the mixing length.

2.2.1.1. *Diagnostic determination of l:* A diagnostic determination of l by simple means was given in section 2.1.2 for mixing length parameterization schemes such as *Blackadar*'s [1962] (Table 2). However, recent work has sought to develop diagnostic relationships for l to be utilized in TKE closure schemes which incorporate more of the complexities of atmospheric flow. *Duynkerke and Driedonks* [1987] distinguish three different length scales and use an interpolation between the three as the diagnostic length scale. In the surface layer the length scale l_B is obtained from the modified Blackadar formulation (6) proposed by *Djolov* [1973]. The limiting value λ in that formulation is the second length scale. It is used in scaling the bulk of the boundary layer [*Mellor and Yamada*, 1974]:

$$\lambda = C_\infty \frac{\int_0^h E^{1/2} z\, dz}{\int_0^h E^{1/2}\, dz} \qquad C_\infty = 0.25 \tag{12}$$

The third length scale (l_s) is that for the stable layer, where

$$l_s = C_s E^{1/2}/N_m \tag{13}$$

and $C_s = 0.36$ and N_m is the Brunt-Väisälä frequency. The mixing length ultimately used by *Duynkerke and Driedonks* [1987] is given as

$$l = \text{Min}\,(l_B, l_s) \tag{14}$$

Beljaars et al. [1987] used a simple mixing length closure in a spectral finite difference model to simulate neutral surface layer flow over complex terrain. They prescribed l in their TKE closure scheme as

$$l = k(z + z_0) \tag{15}$$

where z_0 is the roughness length for undisturbed flow. They concluded that such a simple mixing length parameterization was not valid in attempting to simulate turbulent flow under inhomogeneous conditions. *Therry and Lacarrere* [1983] prescribed an expression for l in terms of altitude and stratification based on the third-order closure scheme of *Andre et al.* [1978] as well as experimental data in convective conditions:

$$\frac{1}{l} = \frac{1}{kz} + \frac{\text{CLK1}}{h} - \left(\frac{1}{kz} + \frac{\text{CLK2}}{h}\right) m_1 m_2 + \frac{\text{CLK5}}{l_s} \tag{16}$$

where CLK1, CLK2, and CLK5 are constants and l_s is the mixing length for stable conditions (see Table 3). *Russell and Takle* [1985] used a modification of *Therry and Lacarrere*'s [1983] formulation for l in the evolution of the stable boundary layer:

$$\frac{1}{l} = \frac{1}{kz} + \frac{1}{l_s} + \frac{1}{\lambda(1 - z/h)} \tag{17}$$

The parameterization of energy dissipation ε in the TKE budget plays an important role in the determination of mixing length. If one chooses to use a diagnostic determination of l as illustrated here (Table 3), then ε in the TKE budget (7) is an unknown and must be modeled. The problem is circumvented by using the generally accepted relationship of *Kolmogorov* [1942]:

$$\varepsilon = C_\varepsilon E^{3/2}/l_\varepsilon \tag{18}$$

TABLE 3. The l Model

Author	l	Range of Validity	Constants
	Diagnostic Determination of l		
Duynkerke and Driedonks [1987]	$l = \min(l_s, l_B)$ $l_s = C_s E^{1/2}/N_m$ $l_B = kz/(\phi_m + kz/\lambda)$	$\partial\theta/\partial z > 0$	$C_s = 0.36$ $C_\epsilon = 0.25$
		$\partial\theta/\partial z \le 0$	$N_m^2 = g\left[\frac{C_{\theta q}\partial\theta_q}{\theta_{q0}\partial z} - C_{qw}\frac{\partial q_w}{\partial z}\right]$ $C_{\theta q} = 1$ unsaturated $C_{\theta q} = (1 + l_v q_{v\,sat})[(1 + q_{v\,sat}\epsilon_r l_v^2)/(c_{pd}R_d T^2)]$
	$\lambda = C_\epsilon\left[\int_0^h E^{1/2} z\,dz / \int_0^h E^{1/2}\,dz\right]$		$C_{qw} = (l_v c_{pd} T)[(1 - \epsilon_r)/\epsilon_r]$ unsaturated $C_{qw} = 1$ saturated $k = 0.4$
Beljaars et al. [1987]	$l = k(z + z_0)$	neutral surface layer	
Therry and Lacarrere [1983]	$\frac{1}{l} = \frac{1}{kz} + \frac{\text{CLK1}}{h} - \left(\frac{1}{kz} + \frac{\text{CLK2}}{h}\right)m_1 m_2 + \frac{\text{CLK5}}{l_s}$		$m_1 = (1 + \text{CLK3}\,h/kz)^{-1}$ $m_2 = [1 - \text{CLK4}(L/h)]^{-1}$ $L < 0$ $m_2 = 0$ $L \ge 0$
	$\frac{1}{l_s}$	unstable	
	$\frac{1}{l_s} = \left(\frac{g}{\theta}\frac{\partial\hat{\theta}}{\partial z}\Big/ E\right)^{1/2}$	stable	CLK1 = 15; CLK2 = 11; CLK3 = 2.5×10^{-3} CLK4 = 1; CLK5 = 3
Russell and Takle [1985]	$\frac{1}{l} = \frac{1}{kz} + \frac{1}{l_s} + \frac{1}{\lambda(1 - z/h)}$	$\partial\theta/\partial z > 0$	$\lambda = \frac{C_4}{h}\int_0^h (qz/f)^{1/2}\,dz$; $q = (2E)^{1/2}$
	$l_s = kL/\beta$		$C_4 = 0.0593$ $k = 0.4$ $\beta = 4.7$
Bodin [1979]	$\frac{1}{l} = \frac{1}{kz} + \frac{1}{0.2h} - \frac{1}{h}\left[\frac{(1 + 1.32z/h)}{0.001 + kz/h}\right]\left(\frac{1}{1 - 50L/h}\right)$	all Ri	see Table 2
	Diagnostic Determination of l_ϵ		
Yu [1976]	$l_\epsilon = kz/(\phi_m + kz/\lambda)$	all Ri	$\lambda = 25m$ $\phi_m = \frac{kz}{u_*}\frac{\partial u}{\partial z}$
Therry and Lacarrere [1983]	$\frac{1}{l_\epsilon} = \frac{1}{kz} + \frac{\text{CLE1}}{h} - \left(\frac{1}{kz} + \frac{\text{CLE2}}{h}\right)m_1' m_2' + \frac{\text{CLE5}}{l_s}$		$m_1' = (1 + \text{CLE3}\,h/kz)^{-1}$ $m_2' = [1 - \text{CLE4}(L/h)]^{-1}$ $L < 0$ $m_2' = 0$ $L > 0$ CLE1 = 15; CLE2 = 5; CLE3 = 5×10^{-3}; CLE4 = 1; CLE5 = 1.5
	$1/l_s = 0$	unstable	
	$1/l_s = \left(\frac{g}{\theta}\frac{\partial\hat{\theta}}{\partial z}\Big/ E\right)^{1/2}$	stable	

Prognostic Determination of l

Busch et al. [1976]	$\frac{\partial l}{\partial t} = \frac{l_s - l}{l/(u_*^2 + w_*^2)^{1/2}}$	h' is the height at which l equals l_B
	$l_s = (kz/\phi_m)(1 - z/h)$	$z \le h'$
	$l_s = l_B$	$z > h'$
	$u_*^2 = l^2\left[\left(\frac{\partial U}{\partial z}\right)^2 + \left(\frac{\partial V}{\partial z}\right)^2\right]$	
	$w_* = \left(\frac{g}{\theta}\overline{w\theta_v}l\right)^{1/3}$	
Mailhot and Benoit [1982]	$\frac{\partial l}{\partial t} = \frac{l_s - l}{l/(u_*^2 + w_*^2)^{1/2}}$	$\partial\theta/\partial z > 0$
	$l_s = h(0.35\xi 1 + 2.5\xi)$	
	$l_s = h(0.35\xi + 5.1\xi^2 - 5.35\xi^3)$	$\partial\theta/\partial z < 0$
	$\xi = \min(z/h, 1)$	

where l_ε is termed the dissipation mixing length. Therefore if one chooses to use a prognostic equation for mixing length, ε is no longer an unknown and need not be modeled.

Implementing (18) into the TKE budget raises an interesting question. Examination of (11) and (18) indicates separate length scales for eddy mixing and dissipation. There has been much discussion concerning the relationship between these mixing lengths [see *Therry and Lacarrere*, 1983; *Detering and Etling*, 1985]. Which length scale should be used, and what is the relationship between the two? The common assumption is that the length scales l and l_ε are equal. *Therry and Lacarrere* [1983] examined several formulations of l_ε and compared them to experimental observations from the Air Mass Transformation Experiment (AMTEX) as well as model and laboratory simulations. They considered the well-known formulation of *Blackadar* [1962] as well as formulations by *Yu* [1976] and *Bodin* [1979] and concluded that none of the formulations account for the wide range of stability encountered in the atmosphere. Instead they proposed an expression for l_ε which agreed better with experimental results:

$$\frac{1}{l_\varepsilon} = \frac{1}{kz} + \frac{\text{CLE1}}{h} - \left(\frac{1}{kz} + \frac{\text{CLE2}}{h}\right)m_1'm_2' + \frac{\text{CLE5}}{l_s} \tag{19}$$

where CLE1, CLE2, and CLE5 are constants and l_s is the mixing length for stable conditions. We include in Table 3 formulations for both l and l_ε. Using a simplified rate equation for $\overline{w^2}$ to obtain an explicit relationship for $\overline{w^2}/E$, *Therry and Lacarrere* [1983] derived a relationship between l and l_ε:

$$l = \left(1 + \frac{g}{\Theta}\overline{w\theta}\, l_\varepsilon/C_\varepsilon E^{3/2}\right)l_\varepsilon \tag{20}$$

Thus, for convective conditions, l is larger than l_ε [*Therry and Lacarrere*, 1983].

The range of application using a diagnostic determination of l emphasizes the importance of properly specifying mixing length. However, it is easy to see that many of these parameterizations are dependent on atmospheric stability conditions and are not applicable for a wide variety of cases. This, of course, is a drawback in the formulation of a diagnostic relationship.

2.2.1.2. *Prognostic determination of l*: An alternative approach in the l model to determining mixing length by diagnostic formulation is to allow l to be time dependent. Such a prognostic equation of mixing length was first formulated by *Shir* [1973] and *Lewellen and Teske* [1973] for second-order modeling. *Busch et al.* [1976] extended the prognostic concept to a simple PBL model. Similarity theory is used in the surface layer, but above the surface layer, *Busch et al.* [1976] reasoned that the evolution of mixing length should depend on two parameters: (1) the strength of boundary layer mixing (characterized by friction velocity u_* and convective velocity w_*) and (2) the difference between actual mixing length l and the value of the mixing length for boundary conditions kept constant at any given time (l_s):

$$\frac{\partial l}{\partial t} = \frac{(l_s - l)}{[l/(u_*^2 + w_*^2)^{1/2}]} \tag{21}$$

where

$$\begin{aligned} l_s &= (kz/\phi_m)(1 - z/h) && z \le h' \\ l_s &= l_B && z > h' \end{aligned} \tag{22}$$

TABLE 4. The E-ε Model

Author	Constants			
	C_2	C_3	C_4	C_5
Duynkerke and Driedonks [1987]	0.09	1.44	1.92	0.77
Beljaars et al. [1987]	0.032	1.44	1.92	0.54
Stubley and Rooney [1986]	0.09	1.44	1.92	0.77
Detering and Etling [1985]	0.026	1.13	1.90	0.77
Modified *Detering and Etling* [1985]	0.026		1.90	0.77
Marchuk et al. [1977]	0.08	1.38	1.40	1.0

For the modified *Detering and Etling* [1985] model C_3 is $1.13l/h$.

and h' is the height at which l_s equals the residual mixing length l_B (h' is taken as roughly h).

Mailhot and Benoit [1982] used the *Busch et al.* [1976] parameterization in a 1-D finite element model but determined l_s from *Blackadar* [1962] and J. W. Deardorff (unpublished manuscript, 1977) formulae for stable and unstable boundary layers, respectively:

$$l_s = h[0.35\zeta/(1 + 2.5\zeta)] \quad \text{stable}$$
$$l_s = h(0.35\zeta + 5.1\zeta^2 - 5.35\zeta^3) \quad \text{unstable} \tag{23}$$

where $\zeta = \min(z/h, 1)$.

There exist relatively few prognostic relationships for mixing length used in TKE closure schemes because the prognostic equation for l is better expressed as a prognostic equation for energy dissipation ε. An equation for ε is more common because the concept of energy dissipation is easier to grasp than that of a mixing length. In addition, using the dissipation equation as an additional prognostic equation eliminates the need for parameterizing ε in the TKE budget. This type of formulation is referred to as an E-ε model and will be considered next.

2.2.2. *E-ε model.* The concept of using a prognostic equation for energy dissipation ε instead of a length scale formulation in the turbulent kinetic energy budget was first proposed among others by *Harlow and Nakayam* [1967], *Daly and Harlow* [1970], and *Hanjalic and Launder* [1972] for fluid engineering applications. The relationship for eddy viscosity in terms of ε can be derived easily from (11) and (18):

$$K_m = C_2 E^2/\varepsilon \tag{24}$$

Therefore calculating ε by means of a prognostic equation is analogous to using a prognostic equation for l. The derivation of the dissipation equation from the equation of motion is quite involved and will not be considered here (see *Lumley* [1980], *Marchuk et al.* [1977], or *Wyngaard* [1975]). Several approximations and parameterizations must be made to obtain the resulting popular form of the simplified equation used in the E-ε model:

$$\frac{\partial \varepsilon}{\partial t} = C_3 \frac{\varepsilon}{E}\left[-\overline{uw}\frac{\partial U}{\partial z} - \overline{vw}\frac{\partial V}{\partial z} + \frac{g}{\Theta}\overline{w\theta}\right] - C_4\frac{\varepsilon^2}{E} + C_5\frac{\partial}{\partial z}\left(K_m\frac{\partial \varepsilon}{\partial z}\right) \tag{25}$$

where the first term on the r.h.s. represents the generation of ε. For modeling purposes the bracketed portion of this generation term is taken in the E-ε model as the maximum of shear production versus shear and buoyancy production, i.e., max (shear, shear + buoyancy) [*Duynkerke and Driedonks*, 1987]. The second term on the r.h.s. represents destruction of ε, and the third term represents the turbulent transport. The constant C_5 is somewhat like an inverse Prandtl number and links eddy viscosity for dissipation to that of momentum, i.e., $K_\varepsilon = C_5 K_m$.

Several researchers have used the E-ε model to describe a variety of atmospheric conditions. There is general agreement on the simplified equation (25) used in the E-ε model but some differences in the constants (as discussed by *Rodi* [1980]). This could be expected because it is through these constants that each modeler strives to "fine tune" his results to those of experimental observations or other model results. Most E-ε models have been used with a standard set of constants derived from engineering applications (see, for example, *Launder and Spalding* [1974]):

$$C_3 = 1.44 \qquad C_4 = 1.92 \qquad C_5 = 0.77 \tag{26}$$

Duynkerke and Driedonks [1987], *Beljaars et al.* [1987], and *Stubley and Rooney* [1986] all used the above constants in E-ε models for boundary layer flow over various terrains and under a variety of stability conditions. The only exception was *Beljaars et al.* [1987], who modified C_5 to 0.54. *Marchuk et al.* [1977] modified the standard E-ε model slightly for the simulation of the oceanic mixed layer and used constants $C_3 = 1.38$, $C_5 = 1.40$, and $C_5 = 1.0$. Table 4 gives a summary of the various constants used in the E-ε models.

A different approach to the determination of constants in the E-ε model was made by *Detering and Etling* [1985]. They considered the E-ε model and its application to neutrally stratified flows in idealized nonrotating boundary layers as opposed to atmospheric boundary layers. Their aim was to develop an E-ε model suitable for atmospheric applications which compared well with atmospheric data. They reasoned that the constants derived from engineering applications for flows in nonrotating boundary layers (equation (26)) were not representative of atmospheric flow in which processes throughout the depth of the boundary layer have an effect on turbulent structure. They applied the standard E-ε model to the atmospheric boundary layer for comparison with observations and a simple mixing length model. Their conclusion from thin shear laboratory flows was that the model with the standard set of constants (26) produced much larger values of u_* and K compared to observations. *Lee and Kao* [1979] in a finite element model of the neutral PBL and *Mason and Sykes* [1980] in a 2-D model simulating vortex roll development also presented similar discrepancies between modeled values of u_* and K and observations. *Detering and Etling* [1985] explained that the difference in values could be the result of the differences in the underlying assumptions and principles upon which the constants in the closure scheme are determined. So instead of the values given in (26), *Detering and Etling* [1985] proposed values for the constants, specifically C_3, which adjust the E-ε model to better simulate the observed structure of the atmospheric boundary layer. Constants C_4 and C_5, equal to 1.90 and 0.77, respectively, are roughly those determined from engineering flows. However, *Detering and Etling* [1985] provide a correction for C_3. It is based on the assumption that C_3 should depend on characteristic length scales of turbulent flow considered. The modification for C_3 is then

$$C_3' = C_3 l/h \tag{27}$$

where l is given by (18) and h is the depth of the boundary layer. This modification is not based on stringent arguments but is proposed simply because it models the observed structure of the boundary layer.

2.2.3. *The E-l model.* A scheme similar to that for the E-ε model is a scheme in which a prognostic equation for the product $E \cdot l$ is used in conjunction with the prognostic equation for turbulent kinetic energy (7). Termed the E-l (or q^2-l) model, it was proposed by *Mellor and Yamada* [1974] as a "model of compromise" between their level 2 and 3 models (hence level 2.5 model). The advantage of the E-l model is that it retains most of the features of a full second-order closure model without the associated complexity. All second-moment equations besides the two prognostic ones are reduced to algebraic equations. It is similar to an E-ε model in that a prognostic equation for l (or ε) is used, but it involves much more of the structure of a second-order model. In this section we consider together the models termed E-l (q^2-l) and level 2.5. E-l models are actually level 2.5 models in which a simplified expression for K has been used [see *Yamada*, 1983]. However, the same prognostic equations are used in both models, and hence they are considered together.

Expressions for turbulent fluxes in the E-l model are obtained from simplifications of the level 2.5 model:

$$\begin{aligned} -(\overline{uw}, \overline{vw}) &= S_m K_m(\partial U/\partial z, \partial V/\partial z) \\ -(\overline{w\theta}, \overline{wq}) &= \alpha S_m K_m(\partial \Theta/\partial z, \partial Q/\partial z) \end{aligned} \tag{28}$$

The exchange coefficient K_m is given by (11), and S_m and α ($=K_h/K_m$) are functions of the flux Richardson number Ri_f [*Yamada*, 1975, 1983] as below:

$$S_m = \frac{1.96(0.1912 - Ri_f)(0.2341 - Ri_f)}{(1 - Ri_f)(0.2231 - Ri_f)} \qquad Ri_f < 0.16$$

$$S_m = 0.085 \qquad Ri_f \geq 0.16 \tag{29}$$

$$\alpha = 1.318(0.2231 - Ri_f)/(0.2341 - Ri_f) \qquad Ri_f < 0.16$$

$$\alpha = 1.12 \qquad Ri_f \geq 0.16 \tag{30}$$

The prognostic equation for the length scale in the E-l model as given by *Yamada and Kao* [1986] for horizontally homogeneous flow is

$$\frac{\partial(E \cdot l)}{\partial t} = C_6 l\left[-\overline{uw}\frac{\partial U}{\partial z} - \overline{vw}\frac{\partial V}{\partial z} + \frac{g}{\Theta}\overline{w\theta}\right] - C_7 E^{3/2}[1 + C_8(l/l_R)^2] \tag{31}$$

where l_R is a measure of the distance away from the wall [*Mellor and Yamada*, 1982] and is modified to include stability effects [*Yamada and Kao*, 1986]:

$$\begin{aligned} l_R &= kz - \mu h[Ri_f/(1 - Ri_f)] \qquad Ri_f < 0 \\ l_R &= kz \qquad Ri_f \geq 0 \end{aligned} \tag{32}$$

with constant μ equal to 0.2. Constants C_6, C_7, and C_8 in (31) are empirically determined from neutrally stratified laboratory experimental data that included channel, pipe, boundary layer, and homogeneous shear flows [*Mellor and Yamada*, 1982]:

$$C_6 = 1.8 \qquad C_7 = 0.06 \qquad C_8 = 1.33 \tag{33}$$

The E-l model generally works well in simulating a wide range of geophysical problems, as shown by *Mellor and Yamada* [1982]. However, *Yamada* [1983] emphasized that based on how the constants (33) are determined, the E-l model might not be as ad hoc as it seems. He considered the complicated closure assumptions originally developed for an E-l equation [*Rotta*, 1951] along with the determination of constants to be major shortcomings in the E-l model. Comparison with turbulence data and other prognostic length scale equations will be helpful in determining the usefulness and efficiency of the E-l model.

3. Comparison of Closure Schemes

In this study, 11 parameterization schemes, chosen as representative of both first-order and TKE closure schemes (given in Tables 1–4), are used for comparison in a one-dimensional model. First-order closure schemes are divided into (1) K profile (*O'Brien*'s [1970] formulation) and (2) mixing length (*Blackadar* [1962], *Djolov* [1973], and modified *Djolov* [1973]) schemes. TKE closure schemes are divided into (1) l model (*Therry and Lacarrere* [1983] formulation for l and l_ε, *Bodin* [1979], and *Duynkerke and Driedonks* [1987]) and (2) E-ε model (constants given in Table 4). The E-l model is not considered for the sake of brevity. For each closure scheme, only the formulation of the eddy viscosity coefficient K_m and associated constants are varied.

3.1. *One-Dimensional Model*

As a means of testing the first-order and TKE closure schemes, numerical simulations of the boundary layer were made using a one-dimensional time-dependent barotropic PBL model originally developed at the Naval Research Laboratory and modified at North Carolina State University to include TKE parameterization schemes. The model consists of prognostic equations given in (3) for U, V, Θ, and Q. There are 30 levels in the vertical (to a height of approximately 3 km) with logarithmic resolution. The numerical scheme is a simple centered-difference in space and forward in time. Fluxes, eddy viscosities, mixing length, and vertical gradients are evaluated at levels midway between the levels at which U, V, Θ, and Q are computed.

Surface layer profiles are assumed valid to the lowest computational level (approximately 45 m) where surface layer similarity is used. Above the surface layer, mixed layer theory based on either first-order or TKE closure is used with eddy coefficient K_m determined by the appropriate relationships given in section 2. Eddy viscosity for heat K_h is a function of K_m and z/L as given by *Businger et al.* [1971]. The dependence on L is a shortcoming of the model because L is a surface variable. For model calculations, PBL height h was given as the lowest level at which local Richardson number exceeded 1.

Lower boundary conditions for E and ε necessary for TKE closure are given as [*Mailhot and Benoit*, 1982]

$$\begin{aligned} E &= 3.75u_*^2 \qquad z/L > 0 \\ E &= 3.75u_*^2 + 0.2w_*^2 + (-z/L)^{2/3}u_*^2 \qquad z/L < 0 \end{aligned} \tag{34}$$

$$\varepsilon = u_*^3/kz \tag{35}$$

where u_* is friction velocity and w_* is convective velocity given as

$$u_* = [(\overline{uw})_0^2 + (\overline{vw})_0^2]^{1/4} \tag{36}$$

$$w_* = [(g/T)h(\overline{wT_v})_0]^{1/3} \tag{37}$$

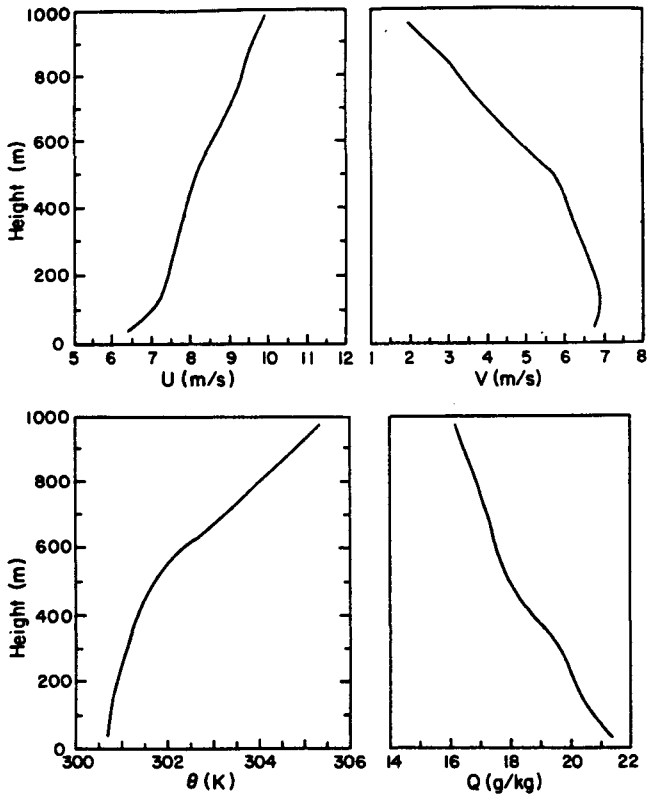

Fig. 2. Profiles used for initialization of the one-dimensional model obtained from MONEX79 radiosonde data.

where subscript zero denotes near-surface values, T_v is virtual temperature, g is gravitational acceleration, and virtual temperature flux $\overline{wT_v}$ is calculated as

$$\overline{wT_v} = \overline{wT} + 0.61\,\bar{T}\,\overline{wq} \tag{38}$$

Upper boundary conditions require $E = \varepsilon = 0$.

3.2. *Data*

Data from the Monsoon Experiment were used in the one-dimensional model simulations. Data were collected from aircraft (mean and turbulence), ship, satellite, and towers in the Bay of Bengal and Arabian Sea regions during MONEX79. Because of limited aircraft data, only one observation day, July 14, 1979, over the Bay of Bengal was chosen here for model simulations. The 1-D model discussed in section 3.1 was initialized at 0000 UT using the mean profiles of U, V, Θ, and Q (Figure 2) obtained from a Soviet ship located in the Bay of Bengal (18.0°N, 89.5°E) and was integrated for a 12-hour period. Unfortunately, monsoon conditions in the Bay of Bengal region during this time period were both nonstationary and inhomogeneous. The monsoon trough had begun to shift northward to the foothills of the Himalayas signaling the beginning of break monsoon conditions. Associated with this shift was a recession of the boundary layer jet and a substantial decrease in wind speed from a maximum of 18 m/s at a height of 1 km at 0600 UT July 13 to 8 m/s at 0000 UT July 14 [*Holt and Raman*, 1987].

To account for the highly variable conditions present on July 14, averaged ship and aircraft data were used to obtain vertical profiles of mean variables U, V, Θ, and Q used in model verification. The 0600 UT soundings from the polygon of stationary Soviet ships centered near 16.2°N, 89.4°E along with the 0400 UT low-level mean aircraft data (19.9°N, 88.9°E) from the NCAR Electra were averaged to obtain mean profiles up to a height of about 1 km. Verification of flux profiles is from Electra turbulence data only. The Electra research flight of July 14 consisted of a vertical "stack" used to study the vertical structure of the monsoon boundary layer.

Sea surface temperature in the region of observations (obtained from ship data) was taken to be a constant 29°C (Θ = 301.7 K) for all model simulations. Geostrophic wind obtained from pressure fields was approximately 16.8 m/s at 233°. The geostrophic wind is an important input parameter in the 1-D model but one which is often difficult to determine accurately. Thus sensitivity of the model to changes in the magnitude of the geostrophic wind is also important and will be considered following the discussion of results.

This monsoon data set was chosen for use in the numerical simulations for two basic reasons: (1) both mean and turbulence structure were readily available and (2) the lack of strong baroclinicity in the boundary layer should make straightforward comparison of different PBL parameterizations to observational data easier to understand. However, the assumption of barotropic conditions in the 1-D model is not entirely representative of the conditions on July 14 as weak horizontal temperature gradients could have existed. Thus, ideally, no closure scheme used in this barotropic 1-D model can be expected to exactly predict the observed structure that would depend on baroclinic effects such as a low-level jet. And as mentioned, the nonstationary monsoon boundary layer also poses problems in determining a representative vertical profile of the region.

For more detailed information on the structure of the boundary layer on this day or the MONEX79 data set, see *Holt and Raman* [1986].

3.3. *Model Results for Different PBL Parameterizations*

3.3.1. *Mean profiles.* There are a variety of ways to systematically and quantitatively measure the accuracy or skill of a model, including root-mean-square (rms) errors, correlation coefficients, bias or threat scores, etc. However, differing conclusions can be drawn depending on the statistical method chosen. As a means of quantifying the comparison of model simulations to observational data, rms errors have been computed from mean profiles for each of the 11 PBL parameterizations (Table 5). Calculations of deviations are made at nine levels:

$$\text{rms} = [\textstyle\sum (O_n - P_n)^2/(n-1)]^{1/2} \tag{39}$$

where O_n is observations at level n and P_n is predicted model value at level n, where $n = 0.1, 0.2, \cdots, 0.9$ km. The rms errors provide an overview of the absolute accuracy of a data set. However, they are poor indicators of how well a model predicts the overall structure of a variable [*Anthes*, 1986]. For example, Figures 3 and 4 show the east-west (U) and north-south (V) wind components for MONEX79 observations and model simulations. Model results are divided according to parameterization schemes given earlier. The first-order schemes of *Blackadar* [1962] and *Djolov* [1973] show no jet structure in either the U or the V profiles but generally give the smallest rms errors. This is simply because they approximate a mean fit to the data. The preferable first-order schemes are the modified *Djolov* [1973] or *O'Brien* [1970] schemes in

TABLE 5. Root-Mean-Square Errors

	U, m/s	V, m/s	Θ, K	Q, g/kg
First-Order Model				
Blackadar [1962]	0.99	0.78	1.35	0.99
Djolov [1973]	0.90	0.80	1.42	1.05
Modified *Djolov* [1973]	0.66	1.39	0.33	1.45
O'Brien [1970]	0.55	1.51	0.34	1.64
l Model				
Bodin [1979]	0.94	1.22	0.28	2.25
Therry and Lacarrere [1983]	0.98	1.26	0.29	1.97
Duynkerke and Driedonks [1987]	0.72	1.38	0.24	1.53
E-ε Model				
Beljaars et al. [1987]	1.21	0.99	0.29	2.90
Duynkerke and Driedonks [1987]	1.24	1.05	0.29	2.90
Detering and Etling [1985]	1.15	1.03	0.29	2.74
Modified *Detering and Etling* [1985]	1.26	1.00	0.26	2.78

which a jet structure is predicted (although largely overestimated in the V profile).

Among TKE closure models (i.e., E-ε and l models) there is only slight variation from one parameterization to another. For example, all E-ε and l model parameterizations overpredict the height of the jet in the U profile. Model results indicate a weak jet of 6.0–6.5 m/s at roughly 600–700 m. Observed jet height is approximately 400–450 m. Model results show a well-mixed profile from the surface up to approximately 500 m.

TKE closure schemes perform better in simulating the observed V profile, in which the jet is much less pronounced (Figure 4). Both E-ε and l model results are similar, showing little variation among schemes. Each parameterization overpredicts V by roughly 1.0–1.2 m/s up to the height of the jet maximum. However, the observed V structure and the height of the jet maximum are simulated well.

Figure 5 shows observations and model simulations of potential temperature Θ. E-ε and l model parameterizations predict well the potential temperature structure, although slightly underpredicting mixed layer values by roughly 0.3–0.4 K. Observations from MONEX79 data indicate a PBL height h of approximately 400 m [*Holt and Raman*, 1986]. However, the vertical resolution of observed Θ near the inversion is not as good as near the surface, and thus it is difficult to state definitively that the models overpredict PBL height. All E-ε parameterizations predict h equal to approximately 600 m. Parameterizations with the l model vary in estimating h. *Therry and Lacarrere*'s [1983] parameterization involving mixing lengths l and l_ε gives h equal to 500 m. Schemes of *Bodin* [1979] and *Duynkerke and Driedonks* [1987] predict mixed layer depths of 550 and 590 m, respectively. Table 6 gives values of h for each parameterization as well as other parameters derived from surface variables.

In contrast to the TKE schemes, first-order closure schemes do not model the observed Θ structure as well. This is a major shortcoming of the first-order schemes. The *Blackadar* [1962] and *Djolov* [1973] parameterizations show no temperature inversion but rather a much warmer and more stable boundary layer. This is because their parameterizations do not consider the effect of the inversion, such as the reduced turbulent mixing above the boundary layer. The *O'Brien* [1970] and the modified *Djolov* [1973] parameterizations indicate a cooler and slightly unstable boundary layer. The modeled depth of the boundary layer, as inferred from the potential temperature structure, and the modeled height of maximum winds show a relationship similar to observations. The low-level jet observed during MONEX79 was typically situated at or slightly above the top of the boundary layer. Profiles of resultant wind speed $(U^2 + V^2)^{1/2}$ (not shown here) calculated with both first-order and TKE closure show wind speed maxima located within the transition region between the boundary layer top and the capping stable layer. Strong boundary layer mixing as evident in

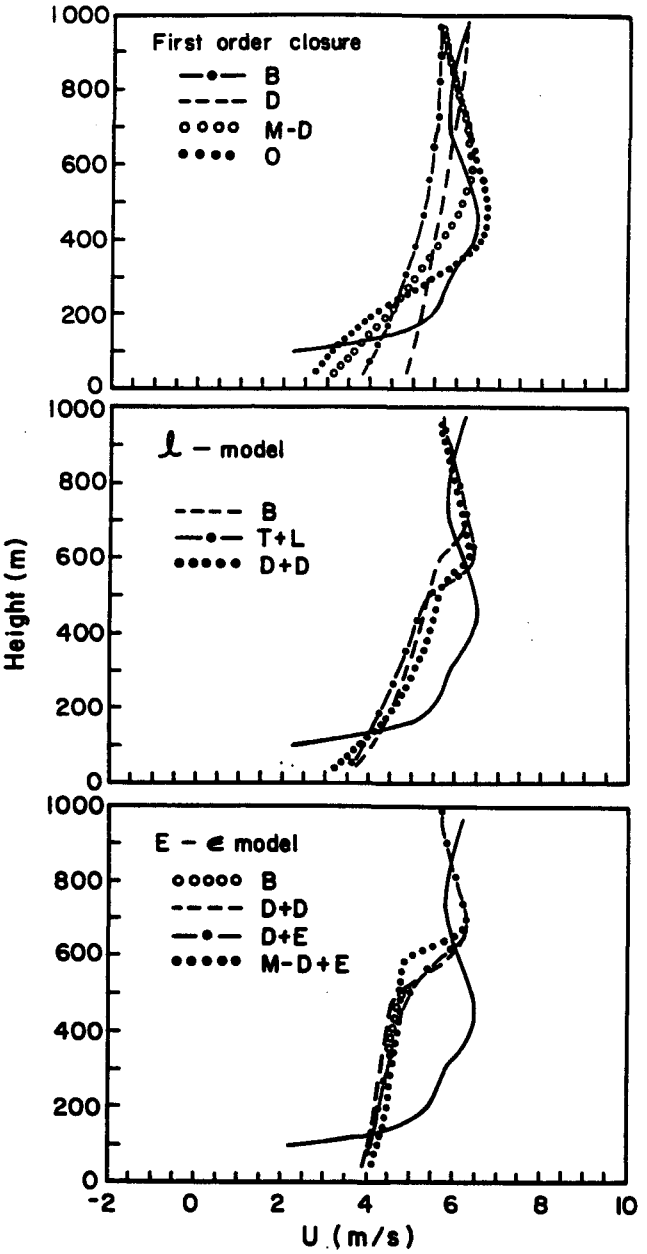

Fig. 3. Vertical profiles of mean east-west wind component U at roughly 0400 UT on July 14, 1979. Solid curves indicate observations obtained from averaged ship and aircraft data. Model simulations are divided according to (*a*) first order closure: *Djolov* [1973] (D); *Blackadar* [1962] (B); *O'Brien* [1970] (O); modified *Djolov* [1973] (M-D), (*b*) *l* model: *Bodin* [1979] (B); *Therry and Lacarrere* [1983] (T+L); *Duynkerke and Driedonks* [1987] (D+D) and (*c*) *E*-ε model: *Duynkerke and Driedonks* [1987] (D+D); *Detering and Etling* [1985] (D + E); *Beljaars et al.* [1987] (B); modified *Detering and Etling* [1985] (M-D+E).

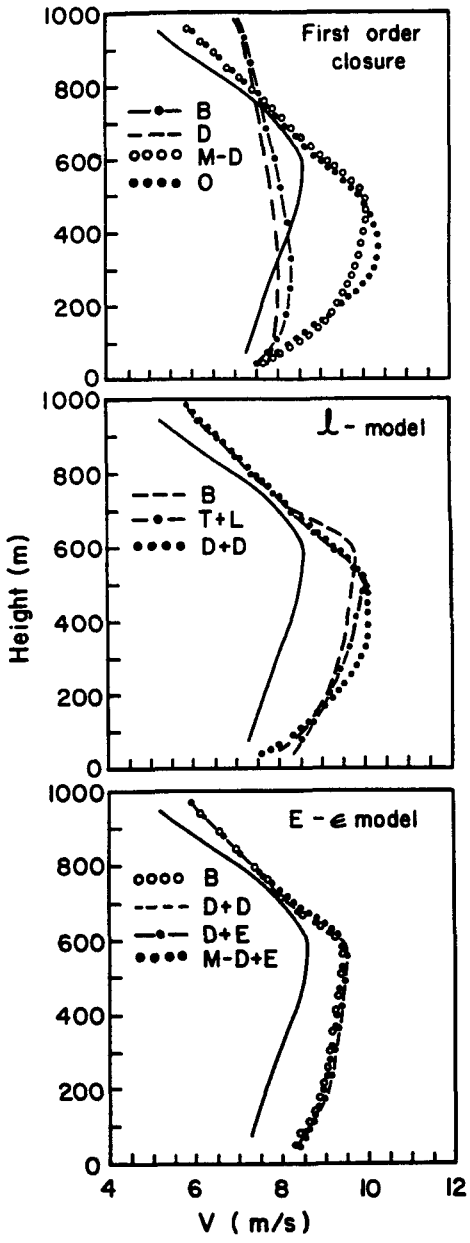

Fig. 4. Same as Figure 3 but for north-south wind component V.

the profile of the eddy viscosity coefficient K_m is important in producing the jet structure and will be discussed later.

Model simulations and observations of specific humidity Q are given in Figure 6. No parameterization does particularly well in predicting the observed Q magnitudes, although TKE models generally simulate the basic structure better in the boundary layer. E-ε and l model parameterizations overpredict Q by 2.0–2.5 g/kg throughout the depth of the boundary layer. The *O'Brien* [1970] and modified *Djolov* [1973] first-order parameterization schemes predict similar values. The large predicted values are probably due to excessive evaporation in the surface layer. Reduction of surface moisture variable q_* by 5–10% gives magnitudes more comparable with observations. The *Blackadar* [1962] and *Djolov* [1973] schemes perform only slightly better near the surface but do not predict the well-mixed profile of Q observed.

The effect of boundary layer mixing on mean profiles can be seen in the profile of eddy viscosity coefficient K_m (Figure 7). Observed values are calculated from (1) and show the well-observed boundary layer maximum at a height between $h/3$ to $h/2$. However, model predictions based on TKE closure, while approximating the basic parabolic structure of K_m, generally do not predict the observed magnitude or height of this maximum. Given the simulated wind profiles, however, K_m is as good as could be expected.

Thus E-ε model parameterizations as well as *Duynkerke and Driedonks* [1987] l model parameterization generate large boundary layer mixing. This is evident in the observed mean profiles, particularly wind profiles in which the jet is situated just above the height of maximum K_m. First-order closure schemes do not predict K_m as well. The *Blackadar* [1962] and *Djolov* [1973] parameterizations show large mixing throughout the depth of the model, as evidenced in the large values of K_m above the boundary layer. The modified *Djolov* [1973]

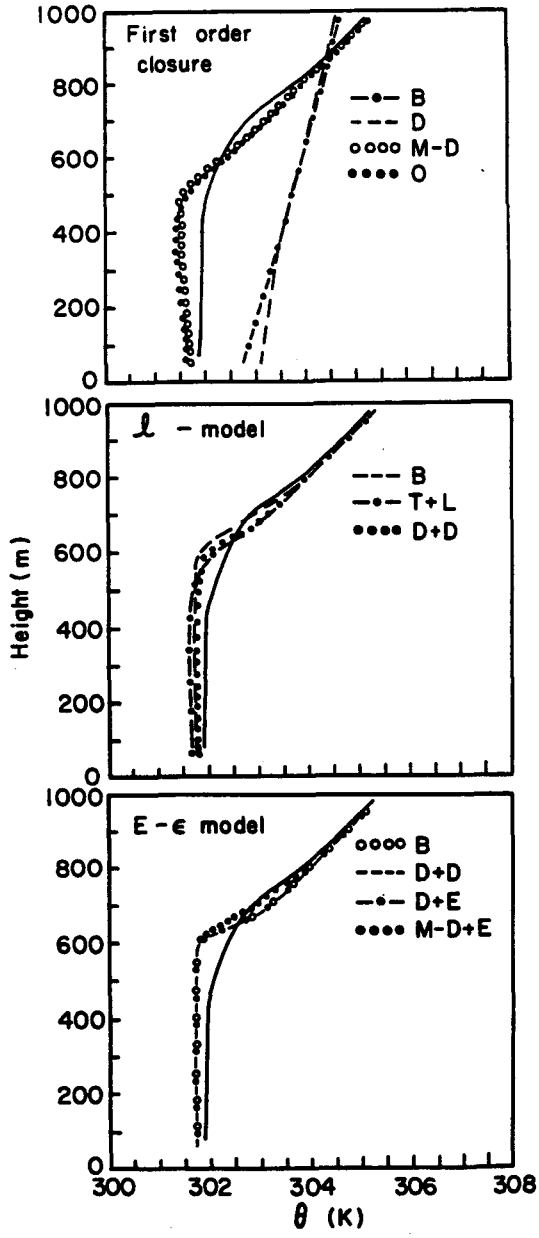

Fig. 5. Same as Figure 3 but for potential temperature.

TABLE 6. Observed and Modeled Boundary Layer Parameters

	h, m	L, m	w_*, m/s	u_*, m/s	θ_*, K
Observed values	400	−255	0.57	0.36	0.025
	First-Order Model				
Blackadar [1962]	···	−570	···	0.247	···
O'Brien [1970]	420	−110	0.628	0.295	0.0289
Djolov [1973]	···	−1050	···	0.240	···
Modified *Djolov* [1973]	480	−95	0.724	0.309	0.0336
	l Model				
Therry and Lacarrere [1983]	500	−106	0.751	0.329	0.0348
Bodin [1979]	590	−108	0.784	0.326	0.0321
Duynkerke and Driedonks [1987]	550	−93	0.749	0.304	0.0314
	E-ε Model				
Duynkerke and Driedonks [1987]	600	−119	0.809	0.346	0.0336
Beljaars et al. [1987]	600	−111	0.808	0.338	0.0335
Detering and Etling [1985]	600	−112	0.808	0.339	0.0335
Modified *Detering and Etling* [1985]	600	−119	0.821	0.351	0.0345

scheme is an improvement in that K_m approaches zero at the top of the boundary layer.

From the comparison of parameterizations for mean values, two main conclusions can be drawn. First, among first-order closure schemes, mixing length parameterizations such as those of *Blackadar* [1962] or *Djolov* [1973], which do not account for effects of the capping boundary layer inversion, do not perform well as compared to schemes which include the effects of reduced mixing above the boundary layer. These mixing length schemes show little agreement with observed mean boundary layer structure. The second conclusion is that among the remaining parameterizations, both first-order and TKE closure, mean variables are relatively insensitive to the closure scheme. Judging from rms errors and the overall predicted mean boundary layer structure, the first-order schemes of *O'Brien* [1970] or modified *Djolov* [1973] or the *l* model or *E-ε* model schemes perform equally well. First-order schemes show smaller rms errors and a closer approximation to the structure in the U and Q profiles, but TKE closure schemes perform better for V and Θ. Other studies [*Duynkerke and Driedonks*, 1987; *Beljaars et al.*, 1987; *Hunt and Simpson*, 1982] have also shown the insensitivity of mean variables to the type of closure scheme.

3.3.2. *Turbulence profiles.* In contrast to mean profiles, turbulence profiles show significant differences among all closure schemes. Figure 8 gives model simulations and MONEX79 observations of the vertical variation of momentum flux for various parameterizations. In general, the *E-ε* model performs best, particularly the modified *Detering and Etling* [1985] parameterization in which constant C_3 is modified to vary with height. All *E-ε* parameterizations do well in predicting near-surface values and the general structure of momentum flux but underestimate throughout the boundary layer. Parameterizations using the *l* model do not predict near-surface values as well as the *E-ε* model (as seen from u_* values in Table 6). Observed values of momentum flux above the top of the boundary layer (about 400 m) show an increase which is not modeled by any parameterization. This increase is probably due to penetrative convection. Both first-order and TKE closure schemes predict momentum flux decreasing to zero at the top of the boundary layer, with the exception of the *Blackadar* [1962] and *Djolov* [1973] mixing length parameterizations which have unrealistic K_m profiles above h.

Observations and model simulations of sensible heat flux $\overline{w\theta}$ are given in Figure 9. Observed heat flux decreases with height from a near-surface value of approximately 0.008 m s^{-1} K, becoming negative in the upper part of the boundary layer. First-order closure has difficulty in simulating the observed heat flux structure, particularly the parameterizations of *Blackadar* [1962] and *Djolov* [1973]. These mixing length parameterizations erroneously predict negative heat flux throughout the boundary layer evident from Θ profiles (Figure 5). Of the TKE schemes, the *E-ε* model performs best in modeling the positive heat flux in the lower half of the boundary layer and the negative flux aloft. The modified *Detering and Etling* [1985] parameterization most closely models the observed structure in the lower boundary layer but surprisingly does worst in predicting the negative heat flux maximum. The *Duynkerke and Driedonks* [1987] *E-ε* parameterization models the negative heat flux well, overestimating by approximately 30% at the top of the boundary layer. The *l* model generally does well in predicting positive heat flux from the surface up to mid–boundary layer depth but as in first-order closure has difficulty modeling the negative flux. *Bodin*'s [1979] parameterization, in which l is diagnostically determined as a function of z/h, has particular difficulty near $z = h$. It greatly overestimates heat flux near the inversion. *Therry and Lacarrere*'s [1983] parameterization is comparable to *E-ε* parameterizations near $z = h$.

Convective temperature θ_* and Monin-Obukhov length L given in Table 6 were calculated as

$$\theta_* = (\overline{wT_v})_0/w_* \tag{40}$$

$$L = -T_v u_*^3/kg(\overline{wT_v})_0 \tag{41}$$

where u_* and w_* were calculated from (36) and (37). Model simulations of friction velocity u_* using TKE closure agree well with MONEX79 observations. First-order closure generally underpredicts u_*, as mentioned earlier. However, first-order closure does better in predicting convective velocity w_* and convective temperature θ_*. This is believed to be due primarily to the inclusion of moisture flux $\overline{wq}$. Figure 10 shows model results and observations of the moisture flux profile. No parameterization does particularly well in predicting the observed magnitude of moisture flux, but near the surface, first-order closure gives the best prediction. *E-ε* and *l*

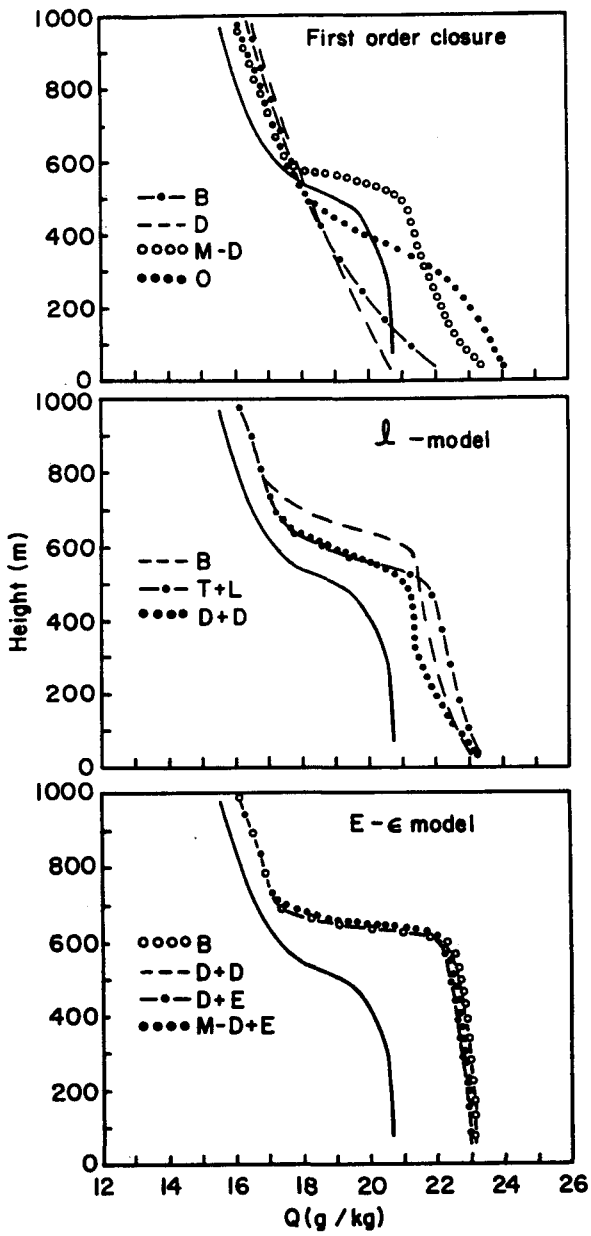

Fig. 6. Same as Figure 3 but for specific humidity.

model parameterizations perform better near the inversion base but generally overpredict in the lower half of the boundary layer. Thus larger $(\overline{wq})_0$ values from TKE parameterizations, as well as deeper boundary layer depth h, result in overprediction of w_*. If one simply considers heat flux with no moisture, TKE parameterizations provide much closer approximations of w_*, θ_*, and Monin-Obukhov length L than first order. This is seen in the heat flux profiles of Figure 9.

Figure 11 shows model simulations and observations of turbulent energy E for E-ε and l model parameterizations. The vertical structure is typical of convective boundary layers [*Deardorff*, 1974]. All parameterizations underpredict near the surface up to approximately 200 m but generally do well above 200 m. The *Duynkerke and Driedonks* [1987] parameterizations for both E-ε and l models show the greatest deviation from other models and from observations.

3.3.3. *Turbulent kinetic energy budget.* Figures 12 and 13 give observations and model simulations of the vertical profile of the budget of turbulent kinetic energy as given by (7). The l model simulations are presented in Figure 12, and E-ε results are given in Figure 13. Solid lines represent MONEX79 observations of buoyancy production (B), shear production (S), dissipation (D), and turbulent transport (T). Similarly, dashed lines represent model simulations. Comparison of the three l model parameterizations given in Figure 12 shows interesting differences. In the lowest 300 m of the boundary layer, all parameterizations indicate shear and dissipation as the dominant source and sink terms, respectively. However, each parameterization greatly overestimates these terms, showing an approximate balance between the two. In contrast, the observed TKE budget shows turbulent transport and dissipation as equally dominant sink terms in the lowest 300 m, balanced by shear and buoyancy near the surface but primarily by shear in the middle of the boundary layer. Buoyancy production is simulated well near the surface, as shown in the discussion of

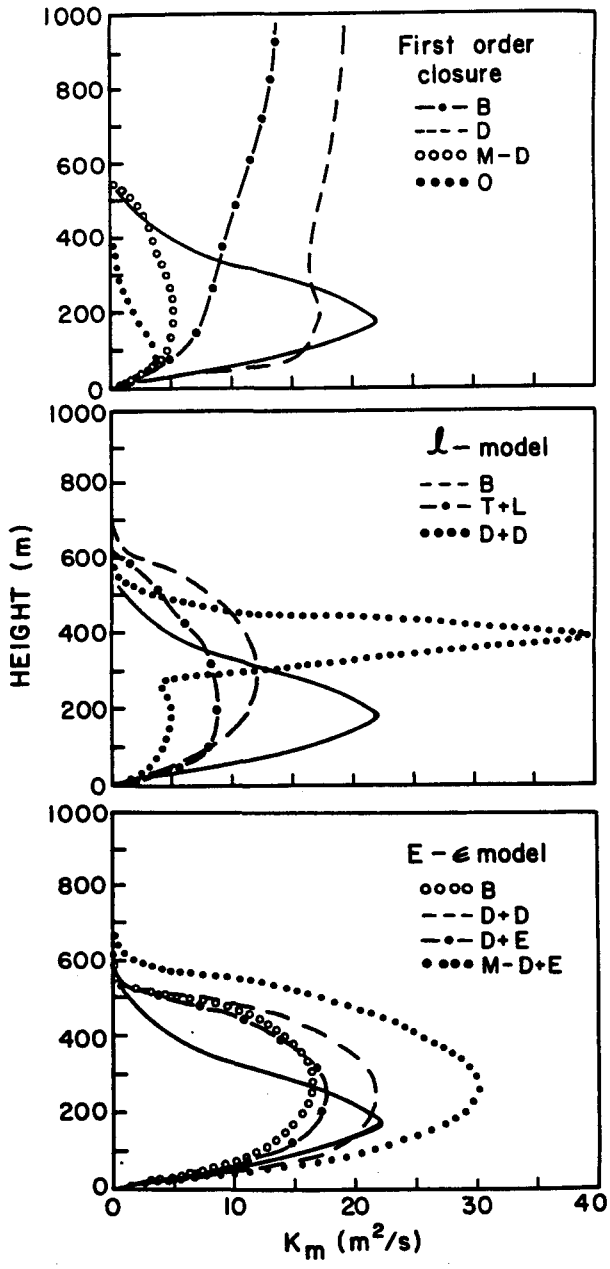

Fig. 7. Same as Figure 3 but for eddy viscosity K_m.

heat flux earlier, but negative fluxes near the inversion are largely overestimated, particularly by *Bodin* [1979]. All three *l* model parameterizations predict transport of TKE from the lower to the upper half of the boundary layer as shown by observations but underestimate the strength of this transport. The height at which turbulent transport changes from upward to downward is modeled well by *Bodin* [1979] and *Duynkerke and Driedonks* [1987] but is underestimated by *Therry and Lacarrere* [1983]. Therry and Lacarrere proposed a correction term for the parameterization of $\overline{wE}$ to account for the upward transport in the lower part of the convective boundary layer:

$$\overline{wE} = -C_k K_m(\partial E/\partial z) + C_E w_*(l_\epsilon/E^{1/2})(g/\Theta\overline{w\theta}) \qquad (42)$$

where C_k and C_E are constants. They showed that this improved parameterization, which included an additional buoyancy production term in comparison to (9), modeled the flux of TKE better and effectively raised the height at which turbulent transport changed sign. This modification was incorporated into *Therry and Lacarrere*'s [1983] original parameterization. Results indicate better agreement with observations for the height at which turbulent transport changes from positive to negative but show only small changes in the magnitude of source and sink terms in the TKE budget. Closer examination of the observed $\overline{w\theta}$ profile indicates that buoyancy flux becomes negative at such a low altitude that it does not strongly influence $\overline{wE}$ for this monsoon boundary layer.

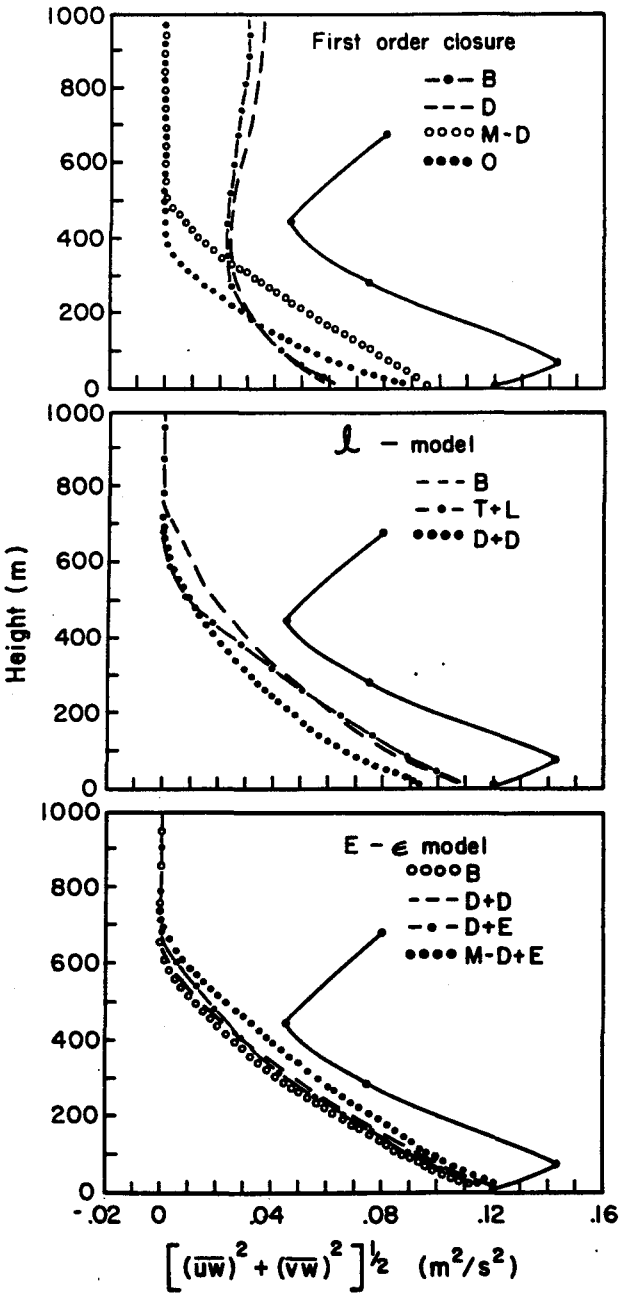

Fig. 8. Same as Figure 3 but for momentum flux. Observational data are from NCAR Electra aircraft data only.

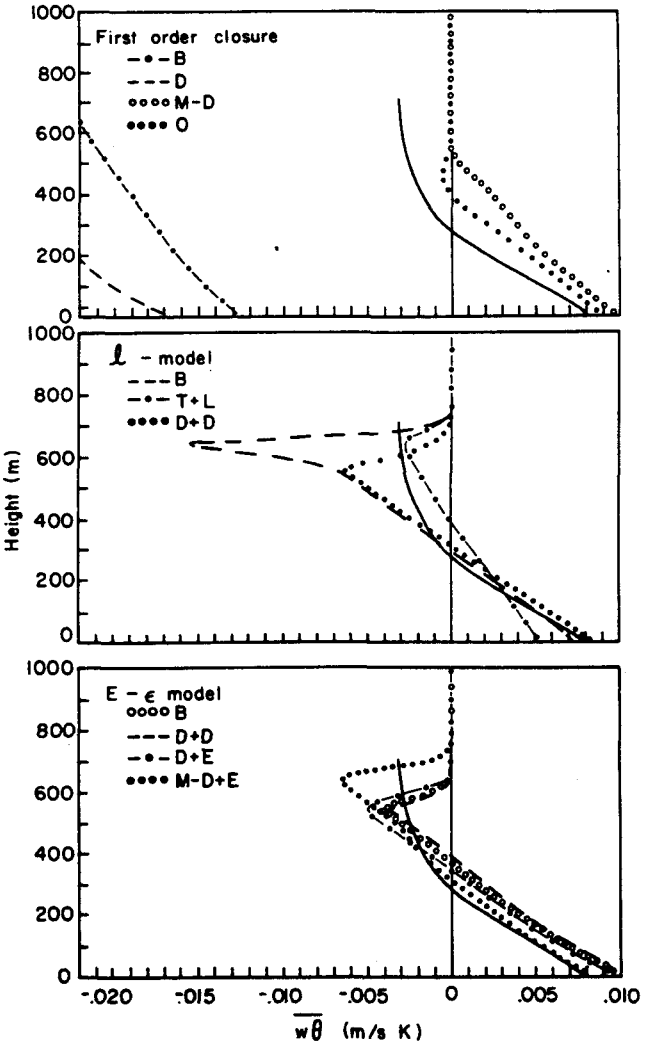

Fig. 9. Same as Figure 8 but for heat flux.

The vertical profiles of dissipation predicted by the *l* model parameterizations (Figure 12) are indications of the sensitivity to mixing length determination. *Therry and Lacarrere*'s [1983] parameterization involving a dissipation mixing length l_ϵ overpredicts dissipation throughout the boundary layer. *Bodin*'s [1979] parameterization is similar to that of Therry and Lacarrere but does better in predicting the vertical structure of ϵ except near the inversion. Of all parameterizations, *Duynkerke and Driedonks*' [1987] simulation of dissipation shows the largest values near the surface. Interestingly, ϵ decreases to zero near 400 m, much lower than observed or predicted by other *l* model parameterizations. Examination of the vertical structure of mixing length (or K_m given in Figure 7) reveals the

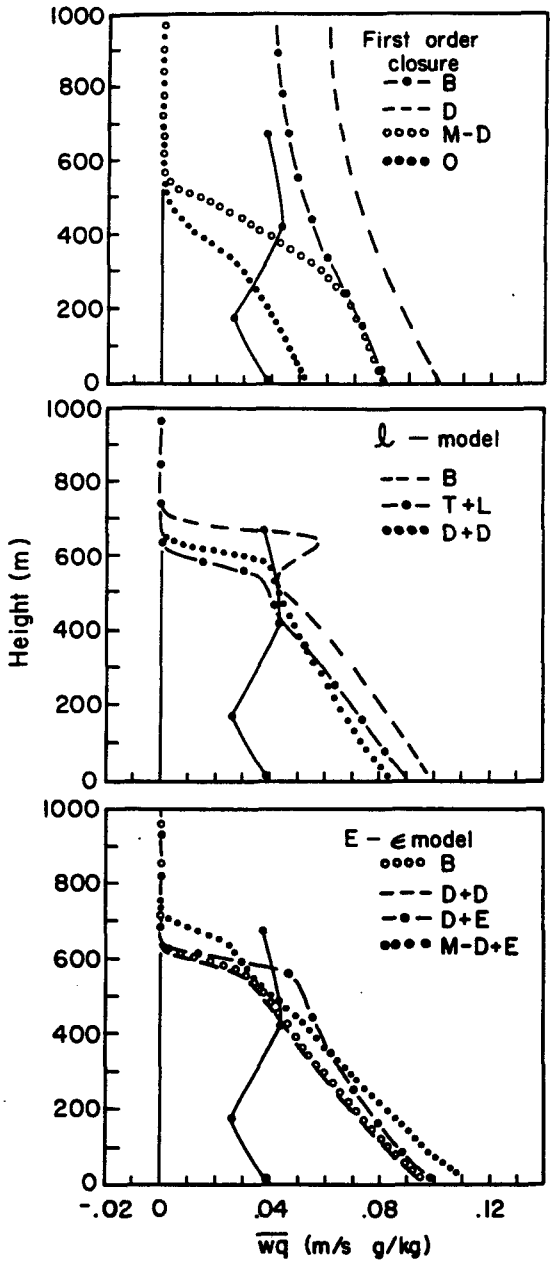

Fig. 10. Same as Figure 8 but for moisture flux.

possible reason. Anomalously large values of K_m and hence l at approximately 400 m in *Duynkerke and Driedonks'* [1987] parameterization cause ε to approach zero. The large mixing length is directly affected by the determination of λ in (12), which Duynkerke and Driedonks assumed to be approximately equal to $h/8$ (about 70 m) for the bulk of the boundary layer. Thus proper determination of mixing length is the major problem in l model parameterizations. One length scale is obviously not suitable either for momentum and dissipation or for an unstable versus stable boundary layer. The inclusion of a prognostic equation for dissipation to replace mixing length appears to be an improvement.

Figure 13 shows the TKE budget for the E-ε model. In comparison to the l model parameterizations shown in Figure 12, profiles predicted by the E-ε model generally show less variation among individual parameterizations. They also show better agreement with observations. This is particularly true for shear and dissipation. All E-ε parameterizations predict the general structure of ε much better than the l model. The modified *Detering and Etling* [1985] parameterization performs best overall, showing the smallest overprediction in both shear production and dissipation. Each E-ε model parameterization underpredicts turbulent transport but does show the general vertical structure, with the exception of *Duynkerke and Driedonks'* [1987] scheme. Their parameterization yields turbulent transport as a source term throughout the boundary layer to compensate for the smaller shear production than that given by other E-ε parameterizations.

4. Model Sensitivity to Initial Conditions

Some mention should be made of the uncertainty or sensitivity of the modeled mean and turbulence profiles. Using the modified *Detering and Etling* [1985] E-ε parameterization, additional simulations were done with the initial geostrophic wind (G) increased and decreased by 25%. Thus simulations were carried out for $0.75G$, G, and $1.25G$. In the 1-D case considered here, the geostrophic wind was the most difficult input parameter to determine. Limited data in the region also made it difficult to accurately predict horizontal and vertical temperature distribution. The $\pm 25\%$ changes were chosen as the maximum and minimum deviations expected in the magnitude of G.

Compared to original model simulations (geostrophic wind

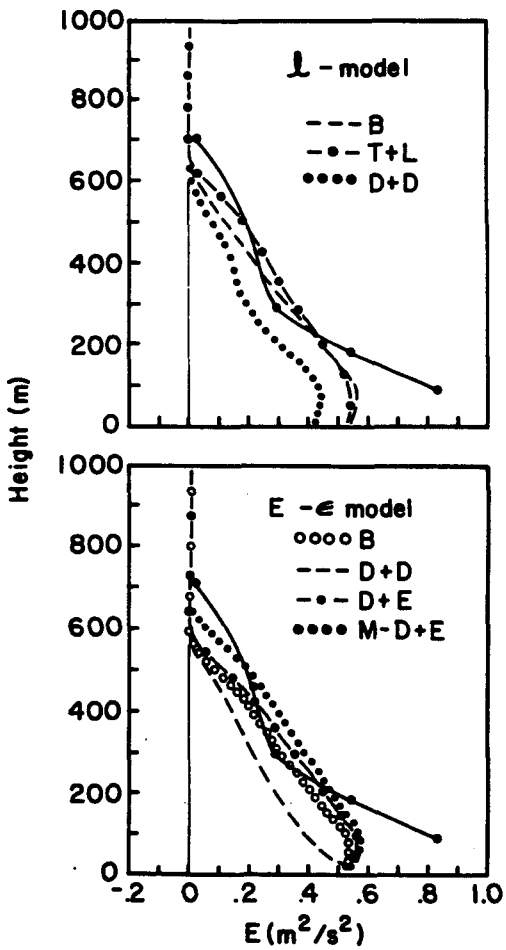

Fig. 11. Same as Figure 8 but for turbulent kinetic energy of l and E-ε models.

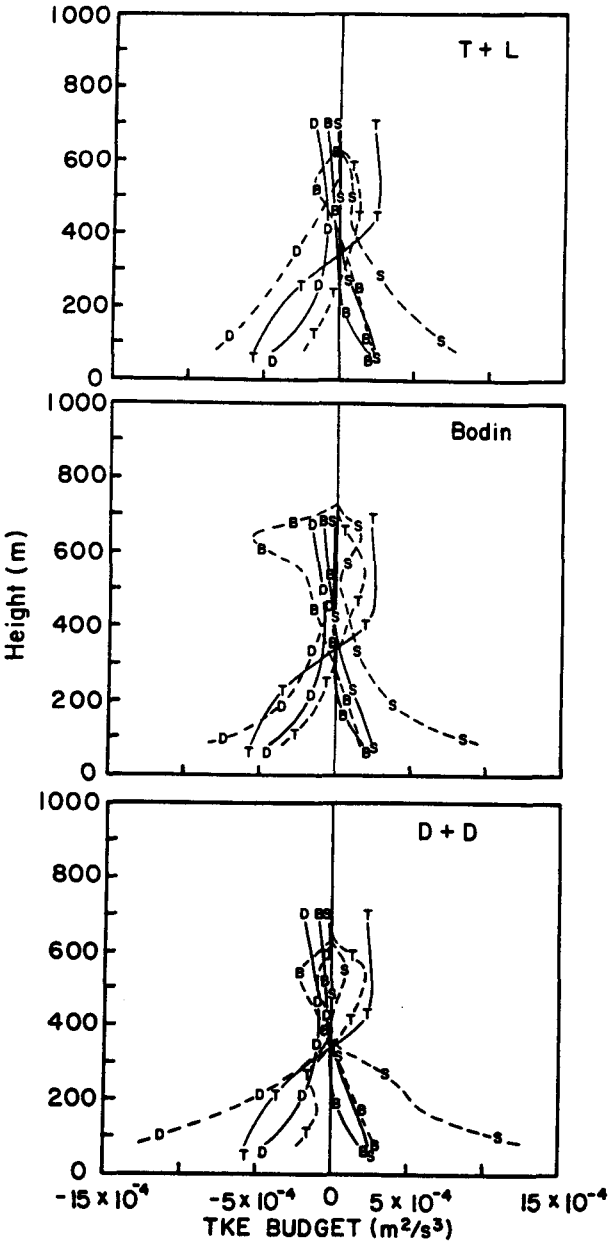

Fig. 12. Vertical profile of the budget of turbulent kinetic energy for the three l model parameterizations given by (top) *Therry and Lacarrere* [1983], (middle) *Bodin* [1979], and (bottom) *Duynkerke and Driedonks* [1987]. Solid curves represent observations of shear production (S), buoyancy production (B), dissipation (D), and turbulent transport (T). Dashed curves similarly represent model simulations.

of 1.0 G), model results at 0400 UT for $\pm 25\%$ changes in G indicated that wind components U and V, turbulent kinetic energy E, and momentum flux showed the largest deviations. Near the surface (up to about 100 m), $\pm 25\%$ changes in G resulted in ± 20–22% changes in the magnitude of U and V and $\pm 28\%$ changes in E. Momentum flux changed by approximately $\pm 32\%$. Near the height of the wind speed maximum (about 600–700 m), changes in U had reduced to $\pm 14\%$, and changes in E had reduced to $\pm 21\%$, while changes in V and momentum flux had remained approximately constant at $\pm 23\%$ and $\pm 29\%$, respectively. Temperature and moisture variables indicated much smaller variations in both mean (about ± 0.1–0.2%) and turbulence (± 7–11%) throughout the boundary layer. Thermodynamic variables are less directly affected by G as evidenced from the PBL equations (3). Variation of mean and turbulent quantities of potential temperature and moisture is dependent primarily on K. Variations in K for $\pm 25\%$ changes in G were approximately $\pm 9\%$ throughout the boundary layer.

The conclusion drawn from these simulations is that reasonable model results are dependent on the accuracy of the initial conditions, such as the geostrophic wind. For $\pm 25\%$ changes in G, differences in model simulations are larger than differences between model versions in the l model or E-ε groups. This dependency of accuracy on initial conditions is not a new result (see, for example, *Anthes* [1986]). We have sought here only to quantify the uncertainty for this 1-D model. However, the profiles of mean and turbulent parameters showed similar structure, and performance of different parameterization schemes was judged from their ability to predict the known physical mean and turbulent structure of the boundary layer.

We can hypothesize on possible sources of model error. Initial profile data were available only from radiosondes launched from ships (Figure 2). These profiles had a vertical resolution of only 50 mbar (approximately 500 m). In contrast, the vertical resolution of averaged ship and aircraft observations shown in Figures 3–6 was of the order of 100–150 m in the boundary layer. Thus because of poor resolution in the initial profiles, small-scale structures apparent in the observations may be difficult to simulate. This could explain the general overprediction of boundary layer depth h from the potential temperature profiles. Factors not accounted for in the model, such as inhomogeneity, baroclinicity, and intermittent clouds present in the Bay of Bengal, would also cause errors when verifying model profiles against observations.

5. Conclusions

Comparison of observations and 1-D model simulations of mean and turbulence profiles in the monsoon boundary layer using various parameterization schemes provides two general conclusions. First, mean profiles such as potential temperature, humidity, and horizontal wind components show little sensitivity to the type of closure parameterization as long as the effects of turbulent mixing in the boundary layer are properly handled. Thus, for mean profiles of U, V, Θ, and Q, determination of K_m using a diagnostic formulation of l or a prognostic determination of ε makes little difference. However, first-order schemes are sensitive to the atmospheric stability and turbulent mixing in the boundary layer. A fundamental weakness of K profile parameterizations is that they typically must be specified as a function of stability. Thus profiles are given on the basis of stable or unstable conditions, as seen in the work by *Yamamoto et al.* [1973] or *Orlanski et al.* [1974]. Mixing length parameterizations were developed to avoid this stability dependence by specifying a parameterization independent of stability. This was attempted through the concept of a mixing length best illustrated in *Blackadar*'s [1962] parameterization. The problem in formulations such as Blackadar's and *Djolov*'s [1973] lies in the failure of the mixing length to properly include stability effects, particularly at the inversion and above the boundary layer. Thus to properly model boundary layer structure, mixing length parameterizations must include some function of stability in the determination of K_m. This is evident upon comparison of results of

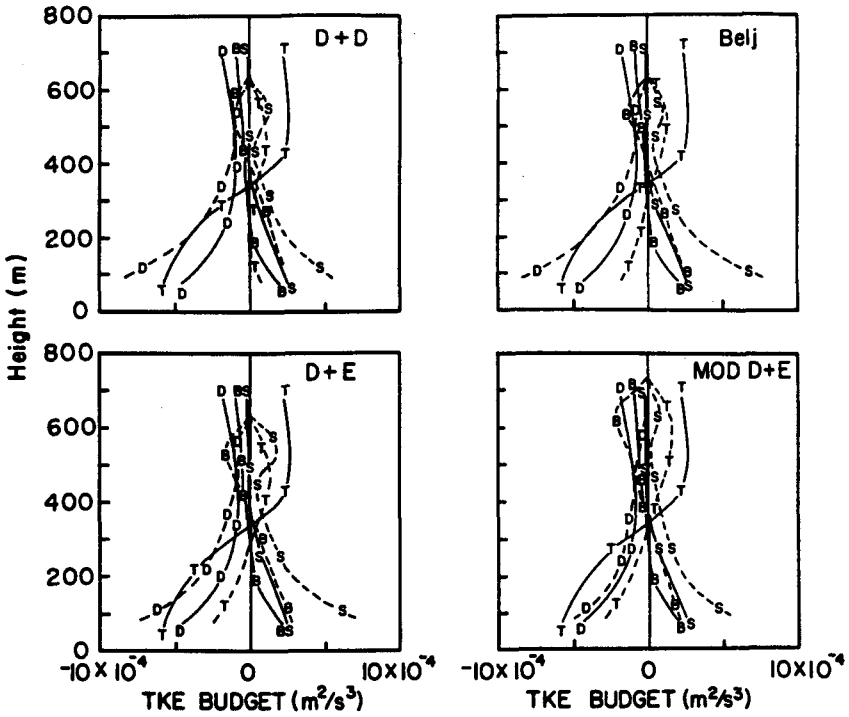

Fig. 13. Same as Figure 12 but for the E-ε model parameterizations of (top left) *Duynkerke and Driedonks* [1987], (top right) *Beljaars et al.* [1987], (bottom left) *Deterling and Etling* [1985], and (bottom right) modified *Detering and Etling* [1985].

the *Djolov* [1973] and modified *Djolov* [1973] schemes, which differ only by a factor equal to $(1 - Ri)^{1/2}$. Above the boundary layer, K_m is reduced to zero in the modified Djolov scheme, as seen in observations, but approaches large positive values for Djolov's original parameterization. Mixing length parameterizations which include stability, such as the modified Djolov scheme or the ones given by *Karlsson* [1972] or *Estoque and Bhumralkar* [1970] show better agreement with observations. Lack of such stability dependence tends to create well-mixed profiles even above the boundary layer.

The second conclusion derived from comparison of model simulations with observations is that TKE closure shows closer agreement with the observed turbulence structure in the boundary layer than first-order closure. Both the magnitude and the vertical structure of momentum and heat fluxes obtained from TKE closure agree better with observations. Among TKE schemes, comparison of vertical flux structures as well as budgets of TKE indicates that, as a group, E-ε parameterizations perform better than l model schemes. Intuitively, this should be true because the E-ε scheme contains more physics of the boundary layer. Also, the E-ε scheme should be able to more accurately predict boundary layer structure from a wider variety of atmospheric cases. This is because it is based on a more physically realistic determination of energy dissipation as opposed to the mixing length determination of the l model schemes. It would be of interest to test PBL parameterizations for differing atmospheric stabilities, not just the convective conditions considered here.

Among E-ε parameterizations the modified *Detering and Etling* [1985] scheme performs best overall. This parameterization differs from other E-ε parameterizations only in the formulation of constant C_3 (dissipation production). The modified constant C_3' given by (27) is generally less than C_3 because l is less than h throughout the boundary layer. Thus production of dissipation in (25) as calculated from the modified Detering and Etling scheme is less than that for the original *Detering and Etling* [1985] parameterization or other E-ε parameterizations given in Table 4. The TKE budget given in Figure 13 reflects this conclusion. Dissipation calculated using the modified Detering and Etling scheme is less than the values for other schemes given and generally shows the closest agreement with observations, but only in the lower part of the boundary layer. The conclusion presented in section 3.3.2 that the modified Detering and Etling scheme has the largest overprediction of negative heat flux near the inversion could also be explained by the dissipation profile. Dissipation near the top of the boundary layer as calculated by modified Detering and Etling approaches zero and is much smaller than the dissipation calculated by other E-ε parameterizations. Thus a larger negative buoyancy production near the top of the boundary layer is required to balance the shear production and the turbulent transport.

It is interesting to note that the modified *Detering and Etling* [1985] parameterization was originally proposed because modeled values of K_m and u_* using the standard E-ε model were larger than observations. Comparison here between E-ε parameterization schemes shows an increase in K_m and u_* for the modified Detering and Etling parameterization. The larger K_m values partly compensate for underprediction of wind shear and generally provide closer agreement with flux observations.

This study has been an attempt to evaluate multilevel PBL parameterizations in a simple 1-D barotropic model. Future research will focus on implementing the improved TKE closure parameterization into a 3-D mesoscale model. Using the Genesis of Atlantic Lows Experiment (GALE) data set, model forecasts will be compared for different boundary layer physics.

Acknowledgments. The one-dimensional model using first-order closure was originally developed at the Naval Research Laboratory by Simon Chang. The authors would like to thank S. Chang for reviewing the manuscript and for useful discussions. This work was supported by the National Science Foundation under grant ATM-83-11812, by the Office of Naval Research under contract N00014-84-K-0620, and by the Naval Research Laboratory, Washington, D. C.

REFERENCES

Andre, J. C., G. DeMoor, P. Lacarrere, G. Therry, and R. Du Vachat, Modeling the 24-hour evolution of the mean and turbulent structures of the planetary boundary layer, *J. Atmos. Sci., 35*, 1861–1883, 1978.

Anthes, R. A., Estimating sensitivity and uncertainty in mesoscale numerical models, paper presented at International Conference on Monsoon and Mesoscale Meteorology, Taipei, Taiwan, Nov. 9–14, 1986.

Arya, S. P. S., Suggested revisions to certain boundary layer parameterization schemes used in atmospheric circulation models, *Mon. Weather Rev., 105*, 215–227, 1977.

Beljaars, A. C. M., J. L. Walmsley, and P. A. Taylor, A mixed spectral finite-difference model for neutrally stratified boundary layer flow over roughness changes and topography, *Boundary Layer Meteorol., 38*, 273–303, 1987.

Blackadar, A. K., The vertical distribution of wind and turbulent exchanges in neutral atmosphere, *J. Geophys. Res., 67*, 3095–3102, 1962.

Blackadar, A. K., High resolution models of the planetary boundary layer, *Adv. Environ. Sci. Eng., 1*, 50–85, 1979.

Bodin, S., An unsteady one-dimensional atmospheric boundary layer model, Proceedings From the WMO Symposium on the Interpretation of Broad-scale NWP Products for Local Forecasting Purposes, Warsaw, October 1976, *Rep. WMO 450*, World Meteorol. Organ., Geneva, 1976.

Bodin, S., A predictive numerical model of the atmospheric boundary layer based on the turbulent energy equation, *SMHI Rep., 13*, Norrkoping, Sweden, 1979.

Bodin, S., Applied numerical modeling of the atmospheric boundary layer, in *Atmospheric Planetary Boundary Layer Physics*, edited by A. Longhetto, pp. 1–76, Elsevier, New York, 1980.

Boussinesq, J., Essai sur la théorie des courantes, *Mem. Pres. Divers Savant Acad. Sci. Paris, 23*, 46, 1877.

Brost, R. A., and J. C. Wyngaard, A model study of the stably stratified planetary boundary layer, *J. Atmos. Sci., 35*, 1427–1440, 1978.

Busch, N. E., S. W. Chang, and R. A. Anthes, A multi-level model of the planetary boundary layer suitable for use with mesoscale dynamic models, *J. Appl. Meteorol., 15*, 909–919, 1976.

Businger, J. A., and S. P. S. Arya, Height of the mixed layer in a stably stratified planetary boundary layer, *Adv. Geophys., 18A*, 73–92, 1974.

Businger, J. A., J. C. Wyngaard, Y. Izumi, and E. F. Bradley, Flux-profile relationship in the atmospheric surface layer, *J. Atmos. Sci., 28*, 181–189, 1971.

Carlson, J. D., and M. R. Foster, Numerical study of some unstably stratified boundary layer flows over a valley at moderate Richardson number, *J. Clim. Appl. Meteorol., 25*, 203–213, 1986.

Clarke, R. H., Recommended methods for the treatment of the boundary layer in numerical models of the atmosphere, *Aust. Meteorol. Mag., 18*, 51–73, 1970.

Clarke, R. H., Attempts to simulate the diurnal cycle of meteorological variables in the boundary layer, *Izv. Acad. Sci. USSR Atmos. Oceanic Phys.*, Engl. Transl., *10*, 360–374, 1974.

Daly, B. J., and F. H. Harlow, Transport equations in turbulence, *Phys. Fluids, 13*, 2634–2649, 1970.

Deardorff, J. W., The countergradient heat flux in the lower atmosphere and in the laboratory, *J. Atmos. Sci., 23*, 503–506, 1966.

Deardorff, J. W., Parameterization of the planetary boundary layer for use in general circulation models, *Mon. Weather Rev., 100*, 93–106, 1972.

Deardorff, J. W., Three-dimensional numerical study of turbulence in an entraining mixed layer, *Boundary Layer Meteorol., 7*, 199–206, 1974.

Deardorff, J. W., The development of boundary layer turbulence models for use in studying the severe storm environment, Open Sesame, in *Proceedings of the Opening Meeting, Boulder, CO, Sept. 4–6, 1974*, edited by D. K. Lilly, pp. 251–264, NOAA, ERL, Boulder, Colo., 1975.

Delage, Y., A numerical study of the nocturnal atmospheric boundary layer, *Q. J. R. Meteorol. Soc., 100*, 351–364, 1974.

Detering, H. W., and D. Etling, Application of the E-ε turbulence model to the atmospheric boundary layer, *Boundary Layer Meteorol., 33*, 113–133, 1985.

Djolov, G. D., Modeling of the interdependent diurnal variation of meteorological elements in the boundary layer, Ph.D. thesis, Univ. of Waterloo, Waterloo, Ont., Canada, 1973.

Duynkerke, P. G., and G. M. Driedonks, A model for the turbulent structure of stratocumulus-topped atmospheric boundary layer, *J. Atmos. Sci., 44*, 43–64, 1987.

Ekman, V. W., On the influence of the Earth's rotation on ocean currents, *Ark. Mat. Astron. Fys., 12*, 1–52, 1905.

Estoque, M. A., and C. M. Bhumralkar, A method for solving the planetary boundary layer equations, *Boundary Layer Meteorol., 1*, 169–194, 1970.

Hanjalic, K., and B. E. Launder, A Reynolds stress model of turbulence and its application to thin shear flows, *J. Fluid Mech., 52*, 609–638, 1972.

Harlow, F. H., and P. I. Nakayam, Turbulence transport equations, *Phys. Fluids, 10*, 2323–2332, 1967.

Holt, T., and S. Raman, Observations of the mean and turbulence structure of the marine boundary layer over the Bay of Bengal during MONEX 79, *Mon. Weather Rev., 114*, 2176–2190, 1986.

Holt, T., and S. Raman, A study of mean boundary-layer structures over the Arabian Sea and the Bay of Bengal during active and break monsoon periods, *Boundary Layer Meteorol., 38*, 73–94, 1987.

Hunt, J. C. R., and J. E. Simpson, Atmospheric boundary layers over non-homogeneous terrain, in *Engineering Meteorology*, edited by E. J. Plate, Elsevier, New York, 1982.

Karlsson, E., A numerical model for the boundary layer of the atmosphere at neutral and stable stratification, *Rep. DM-7*, Inst. of Meteorol., Univ. of Stockholm, Stockholm, Sweden, 1972.

Kolmogorov, A. N., The equation of turbulent motion in an incompressible fluid (in Russian), *Izv. Akad. Nauk SSSR, Ser. Fiz., 6*(1, 2), 56–58, 1942.

Krishna, K., The planetary boundary layer model of Ellison (1956)—A retrospect, *Boundary Layer Meteorol., 19*, 293–301, 1980.

Lacser, A., and S. P. S. Arya, A comparative assessment of mixing-length parameterizations in the stably stratified nocturnal boundary layer (NBL), *Boundary Layer Meteorol., 36*, 53–70, 1986.

Launder, B. E., and D. B. Spalding, The numerical computations of turbulent flows, *Comput. Methods Appl. Mech. Eng., 3*, 269–289, 1974.

Lee, N. H., and S. U. Kao, Finite-element numerical modeling of atmospheric turbulent boundary layer, *J. Appl. Meteorol., 18*, 1287–1295, 1979.

Lewellen, W. S., and M. Teske, Prediction of the Monin-Obukhov similarity functions from an invariant model of turbulence, *J. Atmos. Sci., 30*, 1340–1345, 1973.

Lumley, J. L., Second order modeling of turbulent flows, in *Prediction Methods for Turbulent Flows*, edited by W. Kollmann, pp. 1–31, Hemisphere, London, 1980.

Mailhot, J., and R. Benoit, A finite-element model of the atmospheric boundary layer suitable for use with numerical weather prediction, *J. Atmos. Sci., 39*, 2249–2266, 1982.

Marchuk, G. I., V. P. Kochergin, V. I. Klimok, and V. A. Sukhorukov, On the dynamics of the ocean surface mixed layer, *J. Phys. Oceanogr., 7*, 865–875, 1977.

Mason, R. J., and R. I. Sykes, A two-dimensional numerical study of horizontal roll vortices in the neutral atmospheric boundary layer, *Q. J. R. Meteorol. Soc., 106*, 351-366, 1980.

McBean, G. A., K. Bernhardt, S. Bodin, Z. Litynska, A. P. van Ulden, and J. C. Wyngaard, The planetary boundary layer, *WMO Tech. Note 165*, World Meteorol. Organ., Geneva, 1979.

Mellor, C. L., and T. Yamada, A hierarchy of turbulence closure models for planetary boundary layers, *J. Atmos. Sci., 31*, 1791–1806, 1974.

Mellor, C. L., and T. Yamada, Development of a turbulence closure model for geophysical fluid problems, *Rev. Geophys., 20*, 851–875, 1982.

Monin, A. S., and A. M. Yaglom, *Statistical Fluid Mechanics*, vol. 1, MIT Press, Cambridge, Mass., 1971.

O'Brien, J. J., A note on the vertical structure of the eddy exchange

coefficient in the planetary boundary layer, *J. Atmos. Sci.*, *27*, 1213–1215, 1970.

Orlanski, I., B. B. Ross, and L. J. Polinsky, Diurnal variation of the planetary boundary layer in a mesoscale model, *J. Atmos. Sci.*, *31*, 965–989, 1974.

Panofsky, H. A., and J. A. Dutton, *Atmospheric Turbulence*, 397 pp., John Wiley, New York, 1984.

Pielke, R. A., *Mesoscale Meteorological Modeling*, 612 pp., Academic, New York, 1984.

Pielke, R. A., and Y. Mahrer, Representation of the heated planetary boundary layer in mesoscale models with coarse vertical resolution, *J. Atmos. Sci.*, *32*, 2288–2308, 1975.

Prandtl, L., Meteorologische Anwendungen der Stromungslehre, *Beitr. Phys. Atmos.*, *19*, 188–202, 1932.

Rodi, W., *Turbulence Models and Their Application in Hydraulics*, International Delft, Association for Hydraulic Research, Delft, Netherlands, 1980.

Rossby, C. G., and R. B. Montgomery, The layer of frictional influence of wind and ocean currents, *Pap. Phys. Oceanogr. Meteorol.*, *3*, 101 pp., 1935.

Rotta, J., Statistische Theorie nichthomogener Turbulenz, *Z. Phys.*, *129*, 547–572, 1951.

Russell, R. D., and E. S. Takle, A numerical study of the effects of synoptic baroclinicity on stable boundary layer evolution, *Boundary Layer Meteorol.*, *31*, 385–418, 1985.

Shir, C. C., A preliminary numerical study of atmospheric turbulent flows in the idealized planetary boundary layer, *J. Atmos. Sci.*, *30*, 1327–1339, 1973.

Stubley, G. D., and D. R. Rooney, The sensitivity of k-ε model computations of the neutral planetary boundary layer to baroclinicity, *Boundary Layer Meteorol.*, *37*, 53–70, 1986.

Tag, P. M., and S. W. Payne, Examination of the breakup of marine stratus—A three-dimensional numerical investigation, *J. Atmos. Sci.*, *44*, 208–223, 1987.

Tapp, M. C., and P. W. White, A non-hydrostatic mesoscale model, *Q. J. R. Meteorol. Soc.*, *102*, 277–296, 1976.

Therry, G., and P. Lacarrere, Improving the eddy kinetic energy model for planetary boundary layer description, *Boundary Layer Meteorol.*, *25*, 63–88, 1983.

Wyngaard, J. C., Modeling the planetary boundary layer—Extension to the stable case, *Boundary Layer Meteorol.*, *9*, 441–460, 1975.

Wyngaard, J. C., Boundary layer modeling, in *Atmospheric Turbulence and Air Pollution Modelling*, edited by F. T. M. Nieuwstadt and H. van Dop, pp. 69–106, D. Reidel, Hingham, Mass., 1982.

Yamada, T., The critical Richardson number and the ratio of the eddy transport coefficients obtained from a turbulence closure model, *J. Atmos. Sci.*, *32*, 926–933, 1975.

Yamada, T., Simulations of nocturnal drainage flows by a q^2l turbulence closure model, *J. Atmos. Sci.*, *40*, 91–106, 1983.

Yamada, T., and C.-Y. J. Kao, A modeling study on the fair weather marine boundary layer of the GATE, *J. Atmos. Sci.*, *43*, 3186–3199, 1986.

Yamamoto, G., A. Shimanuki, M. Aida, and N. Yasuda, Diurnal variation of wind and temperature fields in the Ekman layer, *J. Meteorol. Soc. Jpn.*, *51*, 377–387, 1973.

Yu, T. W., Numerical studies of the atmospheric boundary layer with a turbulent energy closure scheme, paper presented at Third Symposium on Atmospheric Turbulence, Diffusion and Air Quality, Am. Meteorol. Soc., Raleigh, N.C., Oct. 1976.

T. Holt and S. Raman, Department of Marine, Earth and Atmospheric Sciences, North Carolina State University, Raleigh, NC 27695.

(Received February 10, 1988;
accepted June 20, 1988.)